Ore Geology Reviews 120 (2020) 103419

Contents lists available at ScienceDirect

Ore Geology Reviews

journal homepage: www.elsevier.com/locate/oregeorev

A genetic relationship between magnesian ilmenite and kimberlites of the Yakutian diamond fields

S.I. Kostrovitsky[a,b], D.A. Yakovlev[a,c], A. Soltys[d], A.S. Ivanov[e], S.S. Matsyuk[f], S.E. Robles-Cruz[g]

[a] Vinogradov Institute of Geochemistry, Siberian Branch of the Russian Academy of Sciences, Irkutsk 664033, Russia
[b] Institute of Earth Crust, Siberian Branch of the Russian Academy of Sciences, Irkutsk, Russia
[c] Irkutsk State University, Geology Department, Irkutsk, Russia
[d] School of Earth Sciences, The University of Melbourne, Parkville, 3010 Victoria, Australia
[e] NIGP AK «ALROSA», Yakutsk, Russia
[f] Semenenko Institute of Geochemistry, Mineralogy and Ore Formation NAS of Ukraine, 34 Acad. Palladina Ave., Kyiv 03680, Ukraine
[g] Algonquin College of Applied Arts and Technology, Ottawa, Canada

ARTICLE INFO

Keywords:
Magnesian ilmenite
Yakutia
Kimberlite
Megacrysts
Xenoliths
Asthenosphere

ABSTRACT

We present new major element geochemical data, and review the existing data for ilmenite macrocrysts, megacrysts, as well as ilmenite in mantle xenoliths from four diamondiferous kimberlite fields in the Yakutian province. This combined data set includes 10,874 analyses of ilmenite from 94 kimberlite pipes. In the studied samples we identify various different ilmenite compositional distributions (e.g., "Haggerty's parabola", or "Step-like" trends in MgO-Cr_2O_3 bivariate space), which are common to all kimberlites from a given cluster, but the compositional distributions differ between clusters. We propose three stages of ilmenite crystallization:

(1) Mg-Cr poor ilmenite crystallising from a primitive asthenospheric melt (the base of Haggerty's parabola on MgO-Cr_2O_3 plots).
(2) This primitive asthenospheric melt was then modified by the partial assimilation of lithospheric material, which enriched the melt in MgO and Cr_2O_3 (left branch of Haggerty's parabola).
(3) Ilmenite subsequently underwent sub-solidus recrystallization in the presence of an evolved kimberlite melt under increasing oxygen fugacity (fO_2) conditions (right branch of Haggerty's parabola in MgO-Cr_2O_3 plots).

Significant differences in the ilmenite compositional distribution between different kimberlite fields are the result of diverse conditions during subsequent ilmenite crystallization in a kimberlite melt ascending through the lithospheric mantle, which have different textures and compositions beneath the studied kimberlite fields. We propose that a TiO_2 fluid formed due to immiscibility of an asthenospheric melt with low Cr and high Ti contents. This fluid infiltrated lithospheric mantle rocks forming Mg-ilmenite. These features indicate a genetic link between ilmenite and the host kimberlite melt.

1. Introduction

Magnesian ilmenite (ilm) is an important kimberlite indicator mineral, which is widely used in diamond exploration to identify primary deposits (e.g., Nowicki et al., 2007). In kimberlites, ilmenite forms discrete monomineralic grains (i.e., megacrysts, macrocrysts, and micro-phenocrysts), whose content varies widely (from 0.1 to 2–3 wt %). Less frequently ilmenite occurs in mantle xenoliths (Rehfeldt et al., 2007; Solov'eva et al., 2019) and in ilmenite-pyroxene intergrowths (e.g., Gurney et al., 1979, Egger, 1983; Clarke and Mackay, 1990). However, the rarity of syngenetic inclusions in ilmenite macrocrysts hampers a complete understanding of the genesis of this mineral. The origin of ilmenite macrocrysts and megacrysts, and their potential genetic relationship with kimberlite magmas and the low-Cr megacryst suite is still debated (Nixon and Boyd, 1973; Jones and Wyllie, 1984; Nowell et al., 2004; Kopylova et al., 2009). Potential origins of ilmenite macrocrysts and megacrysts include:

(I) the disaggregation of ilm-bearing lithospheric mantle lithologies (Blagul'kina et al., 1975; Haggerty, 1975, 2016; Amshinsky et al., 1983; Rodionov et al., 1984; Garanin et al., 1979, 1984; Robles-Cruz et al., 2009); (II) crystallization within the asthenosphere (Boyd & Nixon, 1975; Pasteris, 1979; Harte & Gurney, 1981; De Bruin, 2005; Tappe et al, 2012, 2016); (III) crystallization from an asthenospheric melt within the lithosphere associated with kimberlite magmatism

E-mail address: serkost@igc.irk.ru (S.I. Kostrovitsky).

https://doi.org/10.1016/j.oregeorev.2020.103419
Received 7 August 2019; Received in revised form 28 January 2020; Accepted 17 February 2020
Available online 20 February 2020

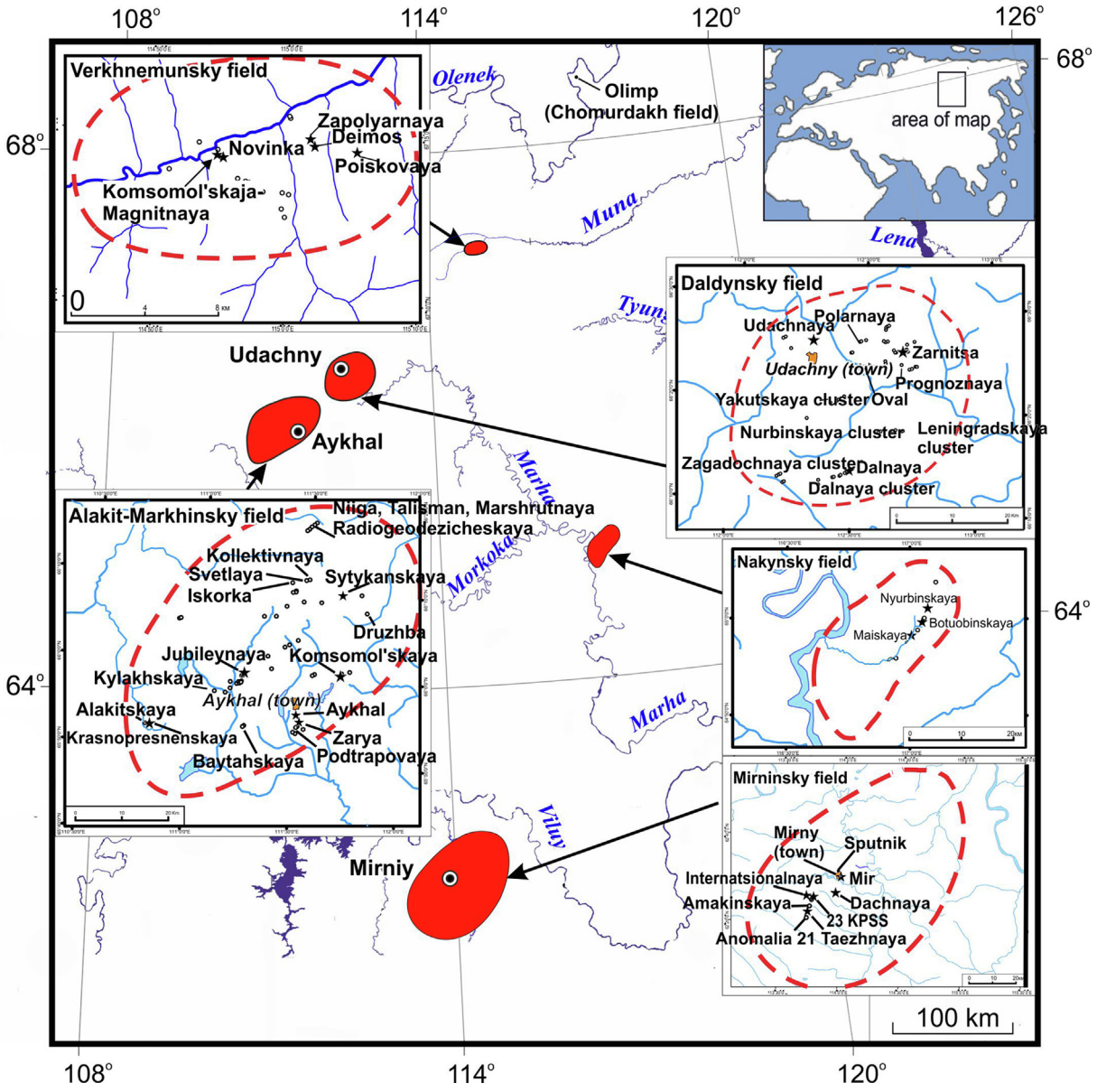

Fig. 1. Map showing the location of diamondiferous kimberlite fields in the Yakutian province. The pipes locations with each field, are reported in Supplementary Fig. 1s-5s.

(Frantsesson, 1968; Frick, 1973; Ilupin et al., 1974, 1978; Gurney et al., 1979; Eggler et al., 1979; Mitchell, 1986; Kostrovitsky, 1986; Nowell et al, 2004; Kopylova et al., 2009; Giuliani et al., 2013; Kamenetsky et al., 2014); a modern take on this previous model is (IV) formation in a "metasomatic aureole" surrounding the (proto-) kimberlite melt and/or previous pulses of failed (proto-)kimberlite melt, alongside other megacryst suite minerals and sheared xenoliths (Moore & Lock, 2001; Moore & Belousova, 2005; Kargin et al., 2017); and (V) crystallisation from other genetically unrelated melts such as basanites, picrites, meimechites and MORB-derived melts (Griffin et al., 1997; Harte, 1983; Jones, 1987; Moore et al., 1992; Tappe et al, 2013, 2015).

We propose that an asthenospheric melt was parental to both kimberlites and minerals of the Cr-poor megacryst suite (including ilm). Convincing arguments are provided by the study of ilmenite compositional distributions within individual clusters, fields, and pipes, as well as the heterogeneity of individual grains. Previously, Mitchell (1986), reviewed the published compositional data on ilmenite from different kimberlite pipes and using factor analysis showed that "*inter-intrusion compositional variations are statistically significant*". Our research not only confirms this, but accounts for the emergence of different compositional distributions of ilmenite from different kimberlite fields, clusters, and pipes.

It is commonly argued that fractional crystallization is the primary mechanism responsible for the formation of composition trends in minerals of the Cr-poor megacryst suite (Mitchell, 1973, 1986; Agee et al., 1982; Moore et al., 1992; Griffin et al., 1997; Moore, 1987); e.g. decreasing NiO contents and Mg# in olivine, increasing FeO_{total} and TiO_2 contents in olivine, garnet, clinopyroxene, and ilmenite. Geochemical data (e.g., incompatible behaviour of Nb in ilm, positive correlation between Ca# in clinopyroxene and Nb in Ilmenite – see Moore et al., 1992), as well as petrographic constraints (e.g., the abundance of clinopyroxene (cpx) inclusions in ilmenite macrocrysts and ilm-cpx intergrowths) indicates that ilmenite and cpx were the final phases of Cr-poor megacryst suite to crystallise (Garanin et al., 1984; Kostrovitsky et al., 2004). However, it remains unclear if fractional crystallization is the only factor which controls the compositional variability of Mg-ilmenite (e.g., increasing MgO and Cr_2O_3 in ilmenite cannot be readily explained by such a process).

The lengthy ascent of kimberlite melts from the deep mantle towards the surface is accompanied by a changes in melt composition, which occurs as a result of the entrainment and partial assimilation of lithospheric material (Agee et al., 1982; Brett et al, 2009; Kamenetsky et al., 2008; Arndt et al, 2010; Russell et al., 2012; Ashchepkov et al. 2014; Soltys et al., 2016, 2018a,b) and changes in redox potential (Eggler, 1983; Mitchell, 1986). Ilmenite is sensitive to such changes (e.g., Green and Sobolev, 1975), and therefore variations in ilmenite composition can be used to elucidate both the genesis of this mineral, and changes in the host kimberlite melt during its ascent through the lithosphere.

In this contribution we summarize the pertinent features of ilmenite compositions acquired during the course of mineralogical assessment of various intrusions in the diamond fields of the Yakutian kimberlite province (YKP). Mineralogical assessment of these intrusions involved the study of ilmenite compositions across four diamondiferous kimberlite fields, covering 94 pipes, and totaling 10,874 analyses thus ensuring the data reported here are representative. Of these analyses 6726 are new, and 4148 have been published previously (Kostrovitsky, 2018).

Here we predominantly focus on bivariate plots of ilmenite composition where one of the axis is the oxide Cr_2O_3, because these charts are the most informative for demonstrating differences between ilmenite from various fields, clusters, and pipes (Haggerty, 1975, 1979; Mitchell, 1986; Moore et al., 1992).

2. Geological setting

The southern portion of YKP contains five diamondiferous kimberlite fields (i.e., Mirninsky, Nakynsky, Daldynsky, Alakit-Markhinsky and Verkhnemunsky) and hosts 20 economic diamond mines (Fig. 1). The majority of these kimberlites are Paleozoic in age (370–350 Ma) based on U-Pb dating of zircons and perovskites (Davis et al., 1980; Kinney et al., 1997; Agashev et al., 2004; Sun et al, 2014, 2018). All these pipes intrude through thick (2.0–2.5 km) sedimentary host rocks consisting of Cambrian-Silurian terrigenous-carbonates (Nowell and Pearson, 1998). These kimberlites contain distinct units with different textures and structures, bulk-rock compositions, as well as diamond and indicator mineral compositions and contents. Most of the studied kimberlites are volcaniclastic or pyroclastic (after Scott Smith et al., 2013). Three chemical groups of kimberlite were distinguished within the studied fields (after Kostrovitsky et al, 2004, 2007): 1) low-Fe-Ti-K (FeO_{total} < 6 wt%, TiO_2 < 1 wt%, K_2O < 1 wt%); 2) low-Fe-Ti, high -K (FeO_{total} < 6 wt%, TiO_2 < 1 wt%, K_2O > 1 wt%); and 3) high Fe-Ti, low-K (FeO_{total} > 6 wt%, TiO_2 > 1 wt%, K_2O < 1 wt%).

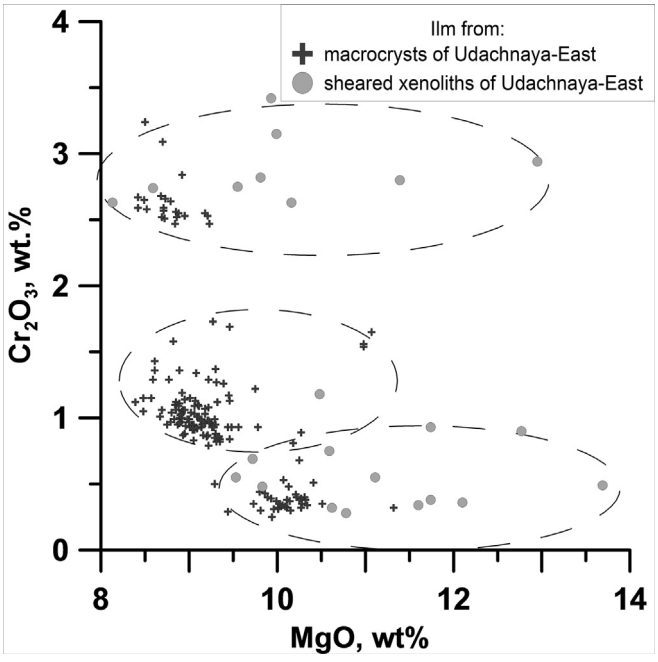

Fig. 2. MgO *vs*. Cr_2O_3 bivariate plot showing the composition of ilm macrocrysts and megacrysts, compared with ilm-bearing xenoliths from the Udacvhnaya-East pipe.

The available data suggests that the petrochemical kimberlite types within the YKP could relate to different mantle source reigons (Bogatikov et al., 2004; Kononova et al., 2005, Blagul'kina, 1975; Milashev, 1965; Kostrovitsky et al, 2004, 2007). The mineral compositions of the studied kimberlites also vary between the different petrochemical, petrographic and textural types of kimberlites. For example, Fe and Ti-rich kimberlites usually contain olivine cores with Mg# = 86–93, and ilmenite is the predominant phase in the heavy mineral concentrates (e.g., Mir, Udachanay-East, Yubileinaya pipes). In contrast, the high-Mg kimberlites contain olivine with Mg# = 85–95, a higher abundance of garnet and Cr-spinel and low concentrations of Ilmenite in heavy mineral concentrates (e.g. Aikhal and Internatsional'naya pipes).

3. Materials, Sampling, and Analytical techniques

Heavy-mineral concentrates were collected from each locality by panning kimberlite material, and ilmenite was subsequently separated from these concentrates by heavy liquid separation. Ilmenite grains then mounted in epoxy for electron probe micro-analyser (EPMA) analysis (~100 grains from each pipe were measured). Electron microprobe analyses were carried out in the Central Analytical Laboratory of the Botuobia Exploration Party ALROSA on a JEOL Superprobe JXA 8230R (Mirniy, Russia, analyst A. Ivanov). Additional analysis were undertaken at the Analytical Common Center at the Institute of Geochemistry, Siberian Branch of the Russian Academy of Science on a JEOL JXA-8200 microprobe (Irkutsk, Russia, analyst L. Suvorova). These electron microprobe instruments are equipped with five energy dispersion spectrometers and analyses were performed at an accelertion voltage of 20 kV, a beam current of 50nA, and counting times were 10 s (peak) and 5 s (background) on both sides of the line.

The composition of ilmenite macrocrysts were determined for most of the kimberlite pipes in the YKP (shown in parentheses is the number of known kimberlite bodies): 1600 analyses from 7 pipes of the Mirninsky field (9), 4148 analyses from 51 pipes of the Daldynsky field (60), 4528 analyses from 25 pipes of the Alakit-Markhinsky field (60), and 598 analyses from 9 pipes of the Verkhnemunsky field (16) (Supplementary Fig. 1s-5s). The compositional heterogeneity of ilmenite macrocrysts was studied on representative polygranular grains from the Mir pipe (Mirninsky field). Of the data discussed in this contribution those from the Mirninsky, Alakit-Markhinsky and Verkhnemunsky (Tables 1s, 3s, 4s in supplementary) fields are new previously unpublished analyses, whereas those from Daldynsky field (Tables 2s in supplementary) have been published in previous contributions by the first author (Kostrovitsky, 2018). Representative examples of zoned ilmenite from the Zarnitsa pipe (Daldynsky field) and Komsomol'skaya pipe (Alakit-Markhinsky field) are provided here to illustrate ilmenite re-crystallization processes (Figs. 7 and 8, Table 2).

To test the hypothesis that ilmenite macrocrysts derive from the disaggregation of peridotitic lithologies we also compare the compositions of ilmenite macrocrysts and ilmenite in sheared peridotites (Table 5s) from the Udachnaya-East kimberlite using previously published data (Sobolev, 1974; Garanin et al., 1984; Solov'eva et al., 1994, Alymova et al, 2004, Solov'eva et al., 2019).

Using the data reported by Solov'eva et al. (2019) we present a brief petrographic overview of two representative ilm-bearing sheared peridotite xenoliths from the Udachnaya-East pipe in order to provide the necessary textural context of these samples (Fig. 11). Finally, we discuss the pressure–temperature parameters of ilmenite crystallization

Table 1
Average, the interval of variation in the composition of Mg-ilmenite from different diamondiferous fields of the Yakutian province (in parentheses - the number of analyses).

	Mirninsky (1600)	Daldynsky (4171)	Alakit-Marhinsky (4634)	Verhnemunsky (5 9 8)
TiO_2	45.8	48.0	48.3	47.4
	28.5–56.5	36.4–55.2	36.7–60.3	37.7–59.5
Al_2O_3	0.6	0.53	0.4	0.5
	0–4	0–1.9	0–1.4	0–3.8
Cr_2O_3	1.0	1.0	1.4	1.4
	0.1–9	0.2–14.5	0–7	0.1–12.6
FeO	18.8	14.4	6.7	15.5
	0–43.4	0.1–44	0–24	0–46.3
Fe_2O_3	24.7	25.8	12.9	26.2
	8–44.5	0.2–45.9	0–30.7	8.9–40.3
MnO	0.16	0.25	0.3	0.2
	0.1–2.4	0.1–2.9	0.1–0.9	0.1–1
MgO	8.8	9.6	9.9	9.1
	0–15.6	0.1–16.2	6–19.7	0.9–18.1

determined by previous studies (based on syngenetic clinopyroxene – Gurney et al., 1979, 1995; Agee et al., 1982; Eggler et al., 1979; Kostrovitsky et al., 2004; Kamenetsky et al., 2009; Sobolev et al., 2015).

4. Results

The compositions of ilmenite megacrysts and macrocrysts from the Mirninsky, Daldynsky, Alakit-Markhinsky, and Verkhnemunsky diamond fields are reported in Supplementary Tables 1s-4. Our mineral chemical data is consistent with previously published data for the limited number of pipes which have been studied (e.g., Zarnitsa and Dalnyaya, Daldynsky field – Amshinsky et al., 1983; Rodionov et al., 1984). This confirms that the analysis reported here are accurate and representative. A literature compilation of the composition of ilmenite macrocrysts and ilmenite in mantle xenoliths from the Udachnaya-East kimberlite is reported in (Supplementary Table 5s).

4.1. Ilmenite macrocryst compositional distributions

Below we review the main ilmenite compositional trends and distributions which are illustrated by plots of MgO (wt.%) *vs.* Cr_2O_3 (wt.%) (Fig. 3). It is important to note that the average composition of ilmenite and its MgO-Cr_2O_3 distribution does not vary with sampling depth, or with the textural type (i.e., unit) of kimberlite within a single pipe. Therefore, the composition of ilmenite is an invariant characteristic unique to a given kimberlite (Kostrovitsky et al., 2003, 2004, 2006; Alymova et al., 2004; Kostrovitsky, 2018).

4.1.1. The Mirninsky field

The Mirninsky field contains two kimberlite clusters orientated NE-SW and spaced ~120 km apart (Fig. 1). These two clusters contain the following pipes: (1) Mir, Sputnik, and Dachnaya; and (2) Internatsional'naya, Amakinskaya, Anomalya-21, Tayozhnaya, 23 KPSS (Fig. 1s).

The ilmenite compositional distribution from both clusters of the Mirninsky field follow the parabola defined by Haggerty (1975) in MgO-Cr_2O_3 space (Fig. 3A). Most analyses of ilmenite from this field are characterized by low Cr_2O_3 contents (< 0.5 wt%) with variable MgO contents (i.e., ~4–14 wt%), forming the base of the parabola. The other

Table 2
Chemical composition of the zoned macrocryst of Ilm from Zarnitsa (see Fig. 7) and Komsomol'skaya pipes (Fig. 8) and polygranular macrocrysts of Ilm from Mir pipe (Fig. 9).

Figures	Fig. 7			Fig. 8				Fig. 9A		
Points	1c	1	1r	1	2	3	4	1	2	3
TiO_2	41.30	50.60	20.54	50.88	52.16	54.41	22.64	48.48	48.48	48.76
Al_2O_3	0.09	0.23	3.24	0.60	0.81	0.54	3.81	0.67	0.68	0.66
Cr_2O_3	0.04	1.18	0.41	0.41	0.77	2.42	1.14	0.17	0.15	0.14
Fe_2O_3	19.68	9.39	–	11.33	9.63	6.28	–	14.47	14.69	15.17
FeO	33.93	22.71	58.32	24.37	22.51	22.61	57.64	28.61	28.85	28.86
MnO	0.16	0.48	0.67	0.24	0.32	0.51	0.84	0.21	0.22	0.20
MgO	1.74	12.47	12.36	11.84	13.76	14.43	13.93	8.29	8.15	8.30
Total	96.94	97.05	95.55	99.67	99.95	101.20	99.99	100.9	101.22	102.09

Figures	Fig. 9A				Fig. 9B				
Points	4	5	6	7	1	2	3	4	5
TiO_2	48.94	52.20	54.74	51.04	38.07	48.28	43.76	49.83	47.76
Al_2O_3	0.73	1.36	0.10	0.05	0.60	0.26	0.69	0.33	0.00
Cr_2O_3	0.15	0.24	0.32	0.42	0.43	0.61	0.46	0.61	0.28
Fe_2O_3	14.52	7.11	5.00	1.01	31.79	14.91	22.51	12.69	4.00
FeO	27.50	27.84	28.77	40.70	25.29	27.14	26.67	26.26	38.19
MnO	0.23	0.36	0.46	4.51	0.16	0.27	0.18	0.33	4.55
MgO	9.13	10.51	11.21	0.35	4.92	8.98	7.01	10.22	0.08
Total	101.2	99.62	100.6	98.08	101.26	100.45	101.28	100.27	94.86

Figures	Fig. 9C		Fig. 9D		Fig. 9E	
Points	1	2	1	2	_1	2
TiO_2	44.05	43.56	32.80	48.01	31.49	48.58
Al_2O_3	0.61	0.69	0.66	0.29	0.55	0.16
Cr_2O_3	0.14	0.19	3.76	5.17	4.15	5.60
Fe_2O_3	22.89	23.16	38.44	11.62	39.81	10.48
FeO	26.95	26.74	22.29	25.40	21.83	25.78
MnO	0.19	0.18	0.13	0.21	0.11	0.36
MgO	6.99	6.87	3.97	9.85	3.57	9.84
Total	101.82	101.39	102.05	100.55	101.51	100.8

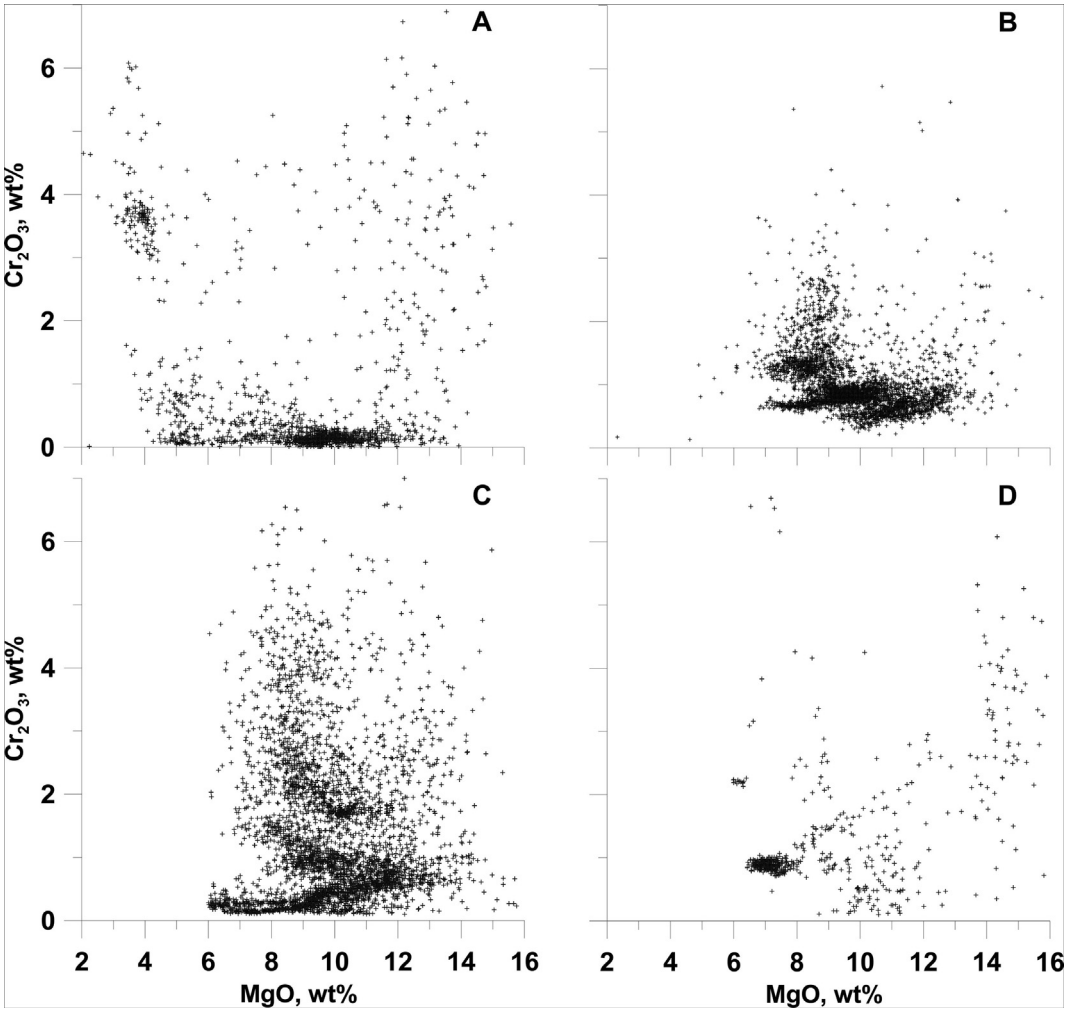

Fig. 3. MgO *vs.* Cr_2O_3 bivariate plots showing the distribution of ilmenite compositions from different diamond-bearing kimberlite fields of the Yakutian province: A - Mirninsky; B - Daldynsky; C - Alakit-Marhinsky; D - Verhnemunsky.

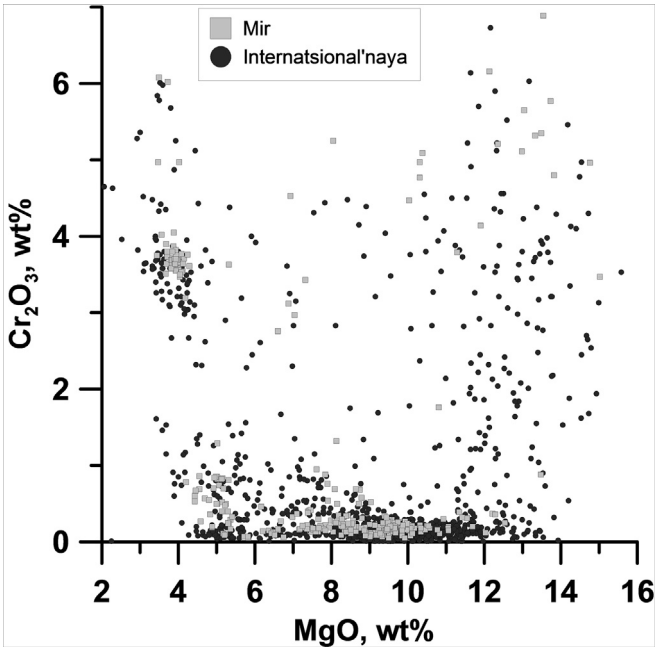

Fig. 4. MgO *vs.* Cr_2O_3 bivariate plots of ilm compositions from two clusters, Mir and Internatsional'naya from the Mirninsky field.

two compositional groups correspond to low- and high-Mg ilmenite with variable Cr_2O_3 contents and generally have a diffuse distribution, forming the two branches of the parabola. However, these two kimberlite clusters exhibit subtle differences in their MgO-Cr_2O_3 distributions, ilmenite from the Internatsional'naya cluster forms a complete parabola, whereas in the ilmenite from the Mir cluster the right branch of parabola is incomplete (Fig. 4). Ilmenite from Mirninsky field is relatively depleted in MgO (Fig. 3, Table 1, Table 1s). Moreover, ilmenite with high hematite component (up to ~43 wt% Fe_2O_3; see also Garanin et al. 1984) typifies the kimberlite field. Indeed, in the 1960's geologist working on the Mirninsky field kimberlites were thrown off, thinking that these ilmenites were in fact magnetite.

4.1.2. The Daldynsky field

The Daldynsky field offers an unrivaled opportunity to study the variation of ilmenite compositions due to the high abundance of ilmenite macrocrysts in the kimberlites of this field (i.e., up to 3 vol%). The Daldynsky kimberlite field is oriented in a NNE-SSW direction and is comprised of 12 pipe clusters as well as several individual pipes (Fig. 2s). The compositions of ilmenite macrocrysts from this field were reported by the first author (Kostrovitsky, 2018). The study of ilmenite compositional distributions within the Daldynsky field (see Alymova et al., 2004; Kostrovitsky et al., 2003, 2006b; Kostrovitsky, 2018) has shown that the ilmenite from a single cluster, have similar compositional distribution patterns and average compositions, yet different clusters show distinct compositional distributions and average

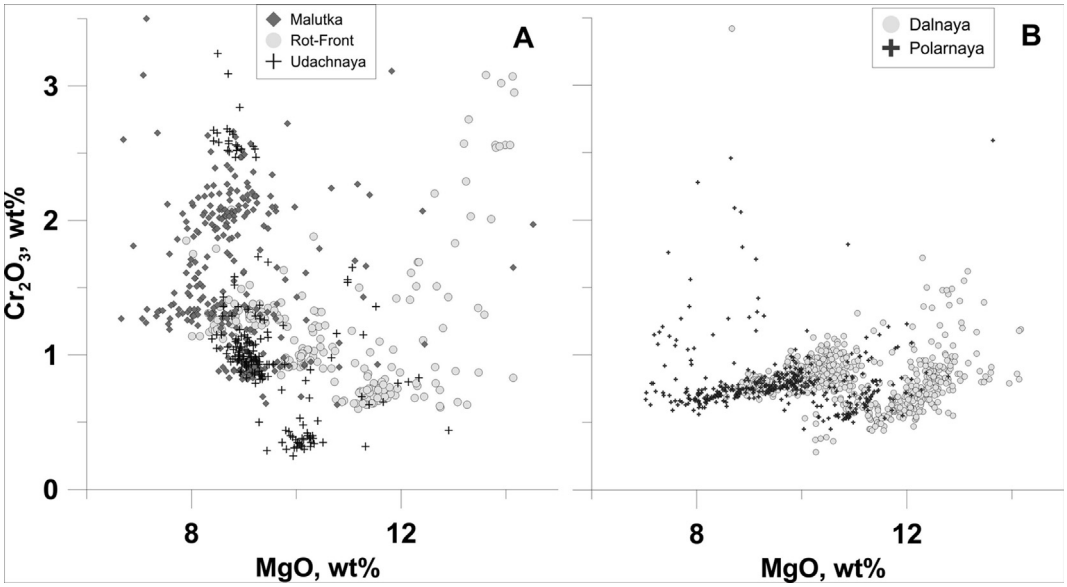

Fig. 5. MgO *vs.* Cr_2O_3 bivariate plots showing the two compositional distribution types of ilm composition from the Daldynsky field: A - "Stepped" for the Zarnitsa cluster; B - "Stepped-inclined" for the Dal'nyaya cluster (see Fig. 1).

compositions (Fig. 3B).

Ilmenite from most clusters of the Daldynsky field (i.e., Zarnitsa, Malyutka, Aeromagnitnaya, Udachnaya, and Yakutskaya clusters) form three distinct groups which can be distinguished based on Cr_2O_3 contents (Fig. 5). This MgO-Cr_2O_3 distribution pattern, which we term "step-like" is not identical for all clusters in the Daldynsky field; the steps differ in both MgO and Cr_2O_3 contents (e.g., Fig. 5A Figure Supplementary Fig. 8s). Similar 'step-like' MgO-Cr_2O_3 distributions have previously been described for ilmenite from the Zarnitsa pipe (Amshinsky et al., 1983; Rodionov et al., 1984). Ilmenite compositional distributions from some other pipes (e.g., the Rot-Front cluster) display combinations of the 'step-like' and 'parabolic' distributions (Fig. 5A).

In contrast, ilmenite from the Polyarnaya and Dalnyaya clusters are characterized by a unimodal Cr_2O_3 distribution (Fig. 5B). Ilmenite from these clusters display two distinctive trends both of which show a positive correlation between MgO and Cr_2O_3: (1) low-Mg Ilmenite (< 10–11 wt% MgO) and (2) high-Mg Ilmenite (> 10–11 wt% MgO). There is no significant correlation between Cr_2O_3 contents and Fe^{3+}/Fe^{2+} ratios (Figure Supplementary Fig. 6s), but there is a positive correlation between MgO and Al_2O_3 (R^2 = 0.63) for ilmenite from Daldynsky field (Figure Supplementary Fig. 7s).

4.1.3. The Alakit-Markhinsky field

The Alakit-Markhinsky kimberlite field is orientated NE-SW and comprises 14 kimberlite clusters as well as individual pipes (Fig. 1, Fig. 3s). The kimberlites in this field are significantly poorer in ilmenite macrocrysts than the Mirninsky and Daldynsky fields. This paucity of ilmenite macrocrysts correlates with a higher bulk-rock MgO content of kimberlites in the Alakit-Markhinsky field (Kostrovitsky et al., 2007). The MgO-Cr_2O_3 distribution of ilmenite from different pipes and clusters of the Alakit-Markhinsky field, show various different compositional distribution trends (Fig. 3C, Fig. 6), including: (a) 'Haggerty's parabola' (Yubileinaya, Kylakhskaya, and Moskvichka pipes) with symmetrical scatter and a wide range of Cr_2O_3 contents (up to 6 wt%); (b) 'hockey stick-like' (three pipes of the Iskorka cluster: Iskorka, Svetlaya, Kollektivnaya), with low Cr_2O_3 contents (predominantly < 1 wt %); (c) "diffuse step-like" (Komsomolskaya, Sitikanskaya, Baytakhskaya, Podtrapovaya, Krasnopresnenskaya, Alakitskaya pipes), with a wide range Cr_2O_3 contents (up to 5 wt%); (d) a combination of "step-like" and 'hockey stick-like' distributions (Druzhba pipe), with low Cr_2O_3 contents (predominantly ≤ 0.5 wt%); and (e) a negative correlation between MgO and Cr_2O_3 contents (3 pipes of NIIGA cluster: NIIGA, Marshrutnaya, Talisman).

4.1.4. The Verkhnemunsky field

The Verkhnemunsky field consists of 16 kimberlite pipes and 4 dykes forming two NW-SE orientated linear chains (Fig. 1, Fig. 4s). All pipes of the Verkhnemunsky field contain a low-Mg Ilmenite group (6.5–8 wt% MgO) which shows a strong correlation between MgO and Al_2O_3 while Cr_2O_3 is constant (Fig. 3D). Ilmenites with such distinctive compositions only occur within this field. Ilmenite from kimberlites of the Verhknemunsky field with an MgO content > 8 wt% show a weak positive correlation between MgO and Cr_2O_3 contents, as well as a distribution similar to "Haggerty's parabola" (Fig. 3D).

In spite of the fact that ilmenite from different kimberlite fields have similar average compositions and wide ranges of major oxide contents (Table 1), ilmenite from different fields show significant differences in their compositional distribution as shown by plots of MgO *vs.* Cr_2O_3. Ilmenite from the Mirninsky field exclusively follows the "Haggerty's parabola" distribution; ilmenite from the Daldynsky field predominantly shows a "step-like" distribution; ilmenite from the Alakit-Markhinsky field displays a combination of several distribution trends (i.e., "Haggerty's parabola", "step-like" and "diffuse"); and ilmenite compositions from the Verkhnemunsky field are characterized by "diffuse" distribution types with one distinctive local area on MgO-Cr_2O_3 plot (Figure Supplementary Fig. 9s).

4.2. Geochemically heterogeneous ilmenite macrocrysts

Most ilmenite grains are heterogeneous, with rims enriched in MgO (up to 14.4 wt%; Fig. 7, Table 2) that are up to 100 μm thick (Elthon & Ridley, 1979; Boctor & Meyer, 1979; Agee et al., 1982; Garanin et al., 1984). For example, SEM-BSE images of a zoned macrocryst from the Zarnitsa pipe (Daldynsky field) and the Komsomol'skaya pipe (Alakit-Markhinsky field) are provided in Figs. 7, 8. This Mg-enrichment is not restricted to concentric rims, but is also recorded in polygranular ilmenite nodules (e.g., Fig. 9). In these nodules individual granules vary in size from 100 μm to > 1 mm and Mg-enrichment extends from grain margins along micro-fractures (Fig. 9 A, B, E, and F). In some examples Mg-enrichment is locally restricted to certain areas within the nodule (e.g., Fig. 9 C, D). Core to rim Mg-enrichment is coupled with Fe_2O_3 depletion, whereas MnO contents increase, and the Cr_2O_3 contents

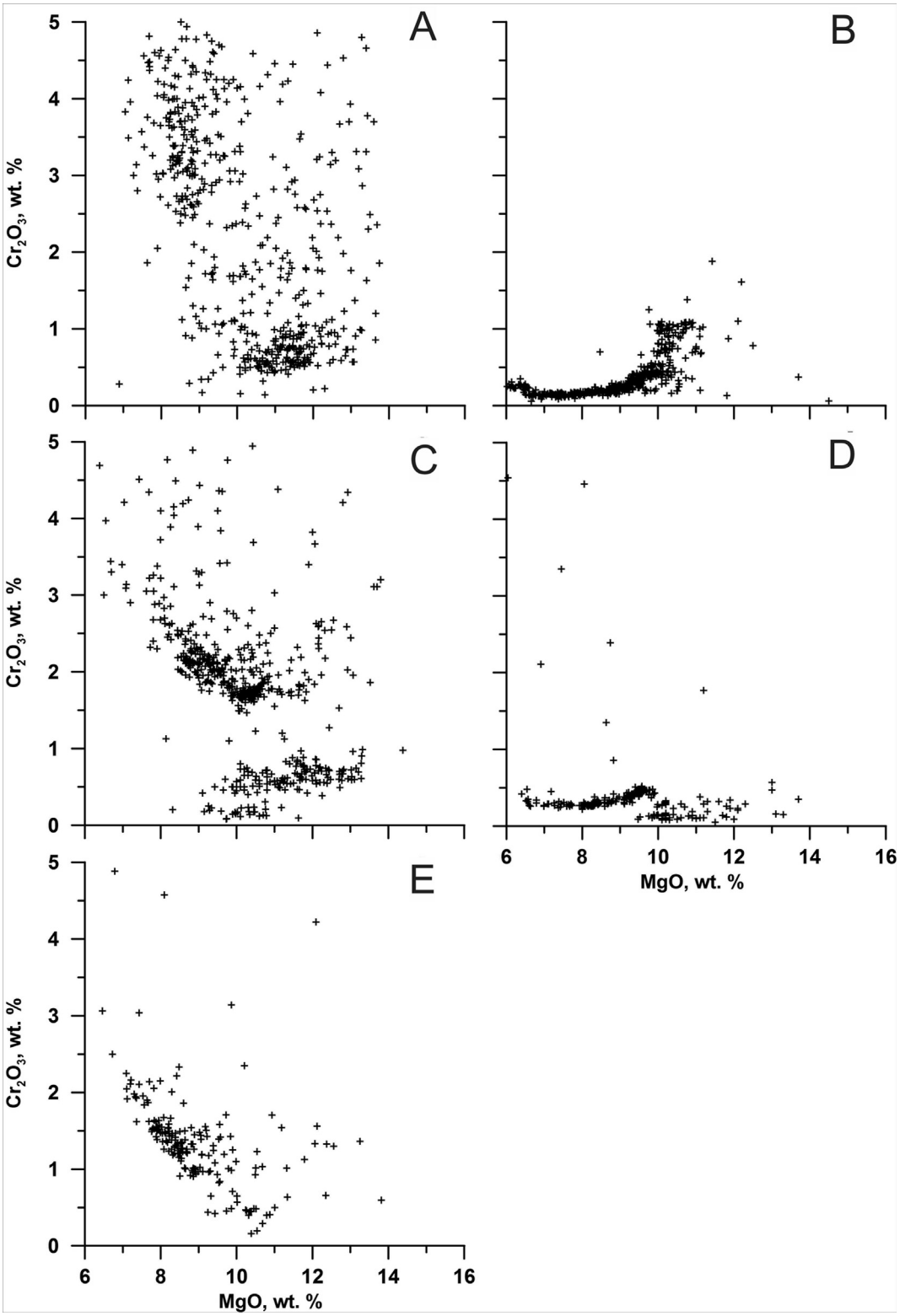

Fig. 6. MgO *vs*. Cr_2O_3 bivariate plots showing the different compositional distribution of ilm from different pipes from the Alakit-Markhinsky field: a) "Haggerty parabola" (Yubileynaya pipe); b) "Hockey stick-like" (three pipes of Iskorka cluster: Iskorka, Svetlaya, and Kollektivnaya); c) "Step-scattered" (Komsomolskaya and Sitikanskaya pipes); d) "Stepped" (Druzhba pipe); e) "Inclined", with an inverse correlation between MgO and Cr_2O_3 (three pipes of the NIIGA cluster: NIIGA, Marshrutnaya, andTalisman).

remain unchanged (Table 2). There is precipitation of Mn-bearing (up to 4.6 wt% MnO) vein-like ilmenite (~30 μm – Fig. 9A - point 7; Fig. 9B - point 5; see Table 2) and Ti-magnetite at the boundaries between individual granules.

The granulation of Ilmenite macrocrysts is the result of re-crystallization, this process causes an increase in the magnesium content while FeO and MnO are removed and re-precipitated beyond the grain boundary where the MnO content of ilmenite may reach 4.6 wt%.

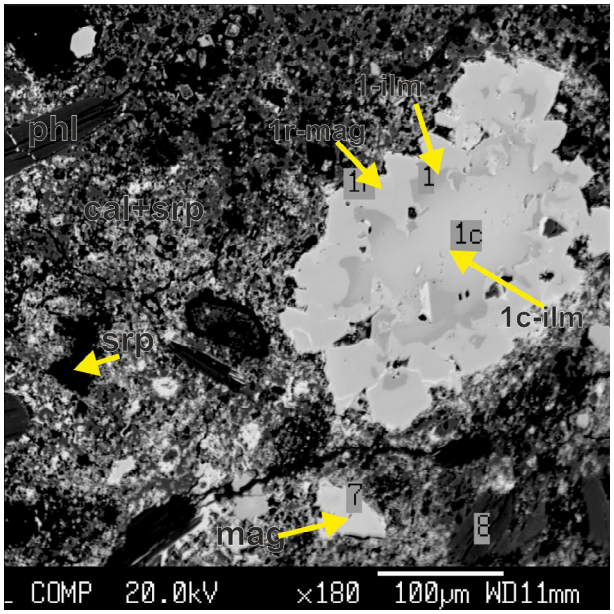

Fig. 7. Back-scattered electron (BSE) image of a zoned ilm grain from the Zarnitsa pipe (Daldynsky field). This ilm grain becomes more magnesian from the core to the rim (see Table 2).

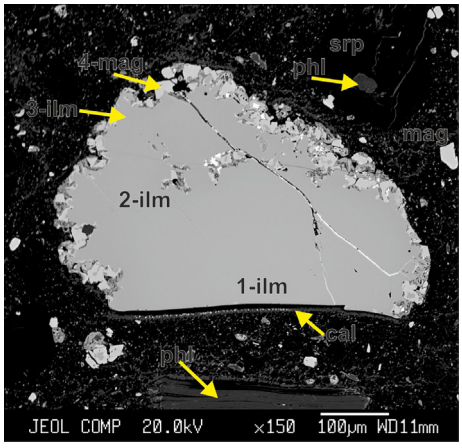

Fig. 8. BSE image of ilm macrocryst from kimberlite of Komsomol'skaya pipe (Alakit-Markhinsky field). In the center, relicts of high-Fe^{+3}, low-Cr Ilm are preserved, the marginal part of the grain recrystallized to relatively high-Mg, high-Cr ilm.

(Table 2, Fig. 9 E, F, G). The MgO content of recrystallized ilmenite macrocrysts varies widely (i.e., from 0.1 to 13.0 wt%), while the Cr_2O_3 contents remain constant across the grain (Fig. 10).

4.3. Ilm-bearing sheared peridotites

The textural features of ilm-bearing sheared peridotites can provide important constraints on the genesis of ilmenite in kimberlites. In most kimberlite localities there is a correlation between peridotite texture (i.e., the degree of deformation) and P-T conditions of equilibration, e.g., Lesotho (Boyd et al., 1997), Jagersfontein (South Africa – Jonston, 1973), Premier (South Africa – Danchin, 1979), Letlhakane (Botswana – Stiefenhofer et al., 1997), and Jericho (Canada – Kopylova et al., 1999). Therefore, it can be assumed that sheared xenoliths are predominantly derived from the lower portions of the lithospheric mantle and equilibrated at higher temperatures relative to granular peridotites (i.e., ~4.5–7 GPa and 1023–1400 °C for sheared xenoliths; e.g., Boyd and Nixon, 1975; Kennedy et al., 2002; O'Reilly and Griffin, 2010; Baptiste et al, 2012; Kargin et al, 2017).

It is noteworthy that the compositions of minerals in sheared peridotites are similar to those of the megacryst suite (Ukhanov et al, 1988; Nixon & Boyd, 1973; Burgess and Harte, 2004; Kostrovitsky et al., 2008; Solov'eva et al., 2008). This similarity has been used to infer a genetic connection between sheared peridotites and the megacryst suite. Below we present a brief summary of the petrographic and geochemical features of two ilm-bearing sheared peridotites (samples 00-83 and UV-218b) from the Udachnaya-East kimberlite, which were described in detail by Solov'eva et al. (2019). The degree of deformation in sheared peridotites is variable and reflected in the rock textures. Porphyroclastic ilm-phl dunites (± minor clinopyroxene) are composed of fine grained olivine neoblasts, coarse olivine porphyroclasts, as well as ilmenite schlieren and phlogopite leists.

Sample 00–83 is an olivine-phlogopite-ilmenite sheared peridotite xenolith with a fluidal porphyroclastic texture as defined by Harte, (1977). This sample contains ~30 vol% olivine (ol), ~40 vol% phlogopite (phl), and ~30 vol% ilmenite. Olivine predominantly occurs as small (0.05–0.2 mm) euhedral neoblasts, but rare anhedral porphyroclasts (< 1 mm) are present. Laminar phl porphyroclasts (< 2 mm) are deformed (i.e., kink-banded) and recrystallized at grain margins. These small recrystallized phl grains are aligned parallel to ilm. Ilmenite occurs as thin lenses (≤0.5 cm wide and ≤ 4 cm long; Fig. 11), which have a polygranular textures (Fig. 12a), resembling the polygranular ilmenite macrocrysts from the Mir pipe described in Section 2.3 (Fig. 9). In a similar manner to the polygranular ilmenite macrocrysts, titaniferous-magnetite has precipitated in the interstitial space between ilmenite granules and at the grain margins of ilmenite lenses. Ilmenite from this xenolith is characterized by wide variations in MgO contents (8.6–12.5 wt%) with relatively constant Cr_2O_3 contents (i.e., 2.6–2.9 wt% –Table 3). Ar^{40}/Ar^{39} dating of phl from this sample yields an age of 367.1 ± 1.4 Ma (Solov'eva et al., 2017), which overlaps the age of host kimberlite (i.e., 367 Ma; Kinny et al., 1997; Yudin et al., 2014).

Sample U-218b is an ol-ilm-cpx sheared peridotite xenolith with a banded porphyroclastic texture. This sample contains ~65 vol% ol, ~30 vol% ilm, and ~5% cpx. Olivine porphyroclasts (0.5–3 mm) occur in a fine-grained mosaic olivine matrix (Solov'eva et al., 2019). Ilmenite grains are 0.3–2 mm in size and are elongated parallel to the samples banding. Rare grains of cpx (0.5–2 mm) are included in ol porphyroclasts and ilmenite bands. Ilmenite in this xenolith is again characterized by a polygranular texture (Fig. 12). Grains of titaniferous-magnetite which are occasionally zoned to Ti-free magnetite occur in the interstitial space between ilmenite granules and at the grain margins of ilmenite bands (Fig. 12b). Ilmenite from this xenolith is characterized by limited variations in MgO contents (10.6–11.8 wt%) with low Cr_2O_3 contents (0.3–0.4 wt%) (Table. 3).

4.4. The composition of ilmenite macrocrysts vs. Ilmenite in mantle xenoliths

Comparison of the compositions of ilmenite macrocrysts (including megacrysts) and ilmenite in sheared peridotites was undertaken using samples from the Udachnaya-East kimberlite (Supp. Table 5S). Based on plots of MgO *vs.* Cr_2O_3 (Fig. 2), there are subtle compositional differences between these two ilmenite populations. Namely, the composition of ilmenite macrocrysts do not extent to as high MgO or Cr_2O_3 contents. Fig. 2 shows that macrocryst compositions can be grouped into three fields clearly distinguished by their Cr_2O_3 content: (1) low-Cr (0.25–0.4 wt%); (2) moderate-Cr (0.75–1.4 wt%); and (3) high-Cr (2.4–2.8 wt%). In contrast, most Ilmenite in sheared peridotites (i.e., 88%) form two sub-horizontal trends stretching along the MgO axis (from 9 to 14 wt%) with narrow ranges of Cr_2O_3 contents (0.3–1.2 wt% and 2.6–3.7 wt%). A subordinate population (22%) form a diffuse cluster with MgO contents of 8–14 wt% and Cr_2O_3 contents 1.43–5.43 wt%.

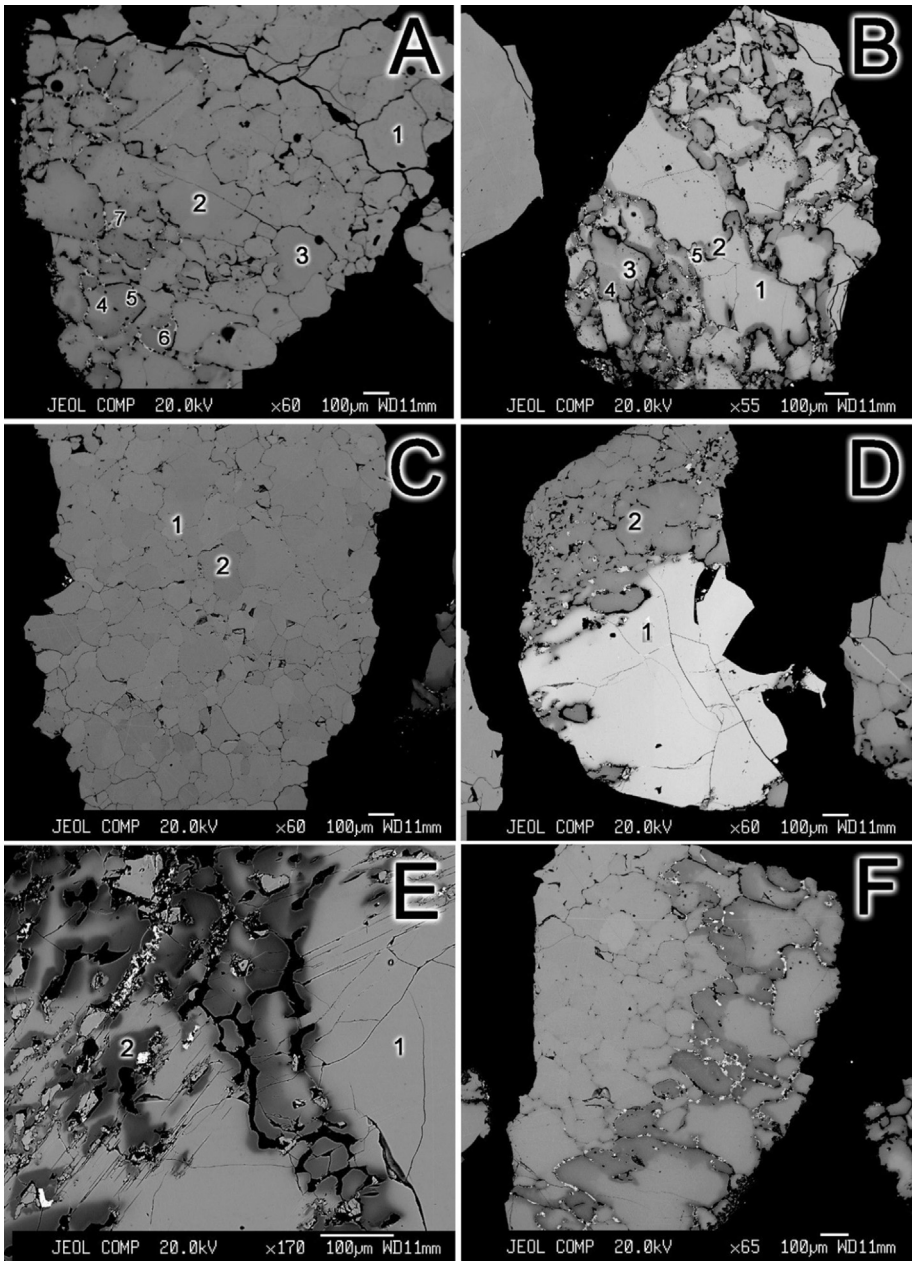

Fig. 9. BSE images of ilm polygranular macrocrysts from Mir pipe (Mirninsky field): A - Uneven granulation of an Ilm macrocryst. The formation of microcracks on the boundaries of granules. B - The changing of Ilm composition is starting in the border zones of granules. C - Relatively uniform micro granulation of ilm grains with the size of individual granules of 100–200 mμ. D - Development of microcracks (granulation process) throughout the macrocrystal ilm, accompanied by a change in composition on only one half of the grain. E, F - The more intensive development of the processes of granulation and substitution takes place in linear microzones of fracturing.

5. Discussion

5.1. The formation of distinct ilmenite compositional distribution patterns

We established 3 stages of ilmenite macrocryst and megacrysts crystallization: 1) asthenospheric; 2) lithospheric; and 3) lithospheric-crust.

It is expected that the first stage of ilmenite crystallization occurred within the asthenosphere (Boyd & Nixon, 1975), together with other minerals of the Cr-poor megacryst suite. A pristine asthenospheric melt had undergone fractional crystallization and, as noted above, was most likely characterized by relatively low Cr and high Fe-Ti contents. Therefore, the primary mechanism for changing the composition of ilmenite as well as other minerals of Cr-poor megacryst suite was fractional crystallization (Mitchell, 1973, 1986; Moore et al., 1992, 2005; Griffin et al., 1997). Ilmenite compositions with variable MgO and relatively low Cr_2O_3 contents (i.e., < 1–2 wt%) on MgO- Cr_2O_3 plots (Fig. 3) illustrate this first stage.

The second stage of ilmenite evolution occurred in response to changes in the composition of the kimberlite melt during ascent through, and interaction with the lithospheric mantle (Agee et al., 1982; Brett et al., 2009; Arndt et al., 2010; Russell et al., 2012; Soltys et al., 2018). The melt was progressively enriched in magnesium and chromium; and therefore, ilmenite compositions evolved in a similar direction. The formation of the left branch of “Haggerty's parabola” (Fig. 3) and plateaux with different Cr_2O_3 contents within the “step-like trend” (Fig. 4) reflect this second stage. There is no correlation between MgO and Cr_2O_3 contents, which can likely be attributed to a high degree of heterogeneity of the melt, that assimilated various lithospheric mantle material (e.g., clinopyroxene, garnet, Cr-bearing spinel).

The third stage of ilmenite evolution is represented by the right branch of “Haggerty’s parabola” in MgO-Cr_2O_3 plots (Fig. 3), and by heterogeneity in individual grains caused by melt oxidation (Figs. 4, 7–10). The “Haggerty’s parabola” distribution is defined by the presence of two ilmenite groups, low- and high-Mg, with identical variation in Cr_2O_3 contents. The right branch of this parabola reflects secondary subsolidus ilmenite recrystallization under changing redox potentials of the evolving kimberlite melt during ascent through the

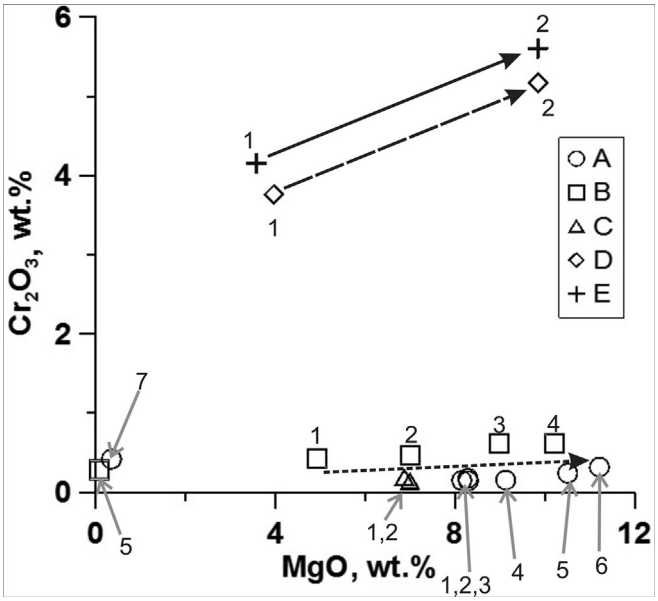

Fig. 10. MgO-Cr_2O_3 plot for polygrainular ilm from the Mir pipe shown in Fig. 9 and reported in Table 2. The letter (i.e., A, B, C, D, E) designates the analysis which correspond to specific macrocryst, and the number shows the location of the spot analysis within this macrocryst (see.

lithosphere, and possibly continuing through to the crust. This process caused increases in the ilmenite MgO content, while Cr_2O_3 contents remain constant. In our view, this process causes the "Haggerty's parabola" distribution in MgO-Cr_2O_3 plots.

MgO-Cr_2O_3 plots show that every kimberlite cluster within a single field displays its own individual ilmenite compositional distribution (Figs. 3, 4). The most common distribution pattern is "Haggerty's parabola" (e.g., ilmenite from the Mirninsky field, and the Yubileinaya pipe of the Alakit-Markhinsky field). The "step-like" distribution is less common and occurs in Ilmenite from pipes of the Daldynsky field and some of the pipes of Alakit-Markhinsky field. These complex distribution patterns cannot be explained by simple fractional crystallization of ilmenite from the kimberlite melt (e.g., Mitchell, 1973, 1986; Moore et al., 1992; Griffin et al., 1997), which would cause decreasing concentrations of compatible elements such as Mg, Cr, Ni, and Sc. Agee et al. (1982) advanced a model, whereby ilmenite compositions change (i.e., toward increasing Mg and Cr contents) with the kimberlite melt composition in response to the assimilation of lithospheric mantle rocks. From Fig. 9s it is evident that ilmenite from Verkhnemunsky field has a distinct compositional distribution from the Daldynsky field, with the former showing less dispersion. Moreover, kimberlites from the Verkhnemunsky field have a significantly lower modal abundance of ilmenite and perovskite.

An important feature of ilmenite compositional distributions is that all kimberlite pipes from the same cluster are characterized by close average ilmenite compositions and the same compositional trends, and *vise versa*, ilmenite from different clusters have different average compositions and compositional trends (see Kostrovitsky et al, 2003; Kostrovitsky 2018). These observations lead us to propose that all kimberlites from the same cluster share a common magma conduit and primitive melt composition, whereas different kimberlite clusters exploit different conduits. Kimberlite melt compositions vary in different feeder channels because of partial assimilation of different lithospheric mantle wall rocks. In turn, evolving kimberlite melt compositions are reflected in the variation of ilmenite compositions.

The compositional heterogeneity of ilmenite macrocrysts (see section 2.4), including poly-granular nodules (Table 2, Figs. 7–10), is expressed by Mg-rich rims and zones along the grain boundaries of recrystallized macrocrysts (Boctor & Boyd, 1977, 1980; Garanin et al., 1984; Agee et al., 1982). We postulate that the recrystallisation of ilmenite macrocrysts occurred in response to stress imparted during their ascent in the host kimberlite melt towards the surface, as a result of changing P-T-fO_2 parameters of the melt. Subsolidus recrystallization of ilmenite resulted in a decrease in Fe^{3+}, a corresponding increase in Mg, Ti and Mn contents, whereas the Cr_2O_3 contents remain constant or slightly increase (Table 2, Fig. 10). The lack of change in the Cr_2O_3 content of ilmenite is explained by a constant composition of the host melt during ilmenite recrystallization caused possibly by the change of fO_2 parameters.

"Step-like" ilmenite compositional distribution patterns reflect changes in the evolution of the host kimberlite melt ascending through the lithosphere. Lithospheric mantle material of different compositions are disaggregated and assimilated by different melts in different conduits. We propose that the formation of two sub-parallel inclined steps (i.e., the positive correlations in low-Mg and high-Mg portions of the MgO-Cr_2O_3 plots for ilmenite from kimberlites of the Dalnyaya and Polyarnaya clusters) was formed by the same process as that which formed the "Haggerty's parabola" trend (Fig. 5).

The trace element compositions of kimberlites from different fields of the Yakutian province indicate a high level of similarity of their asthenospheric source (Kostrovitsky et al., 2007). This asthenospheric melt composition affinity probably resides in the proximity of the average composition of ilmenite (Table 1). In our view, significant differences in ilmenite compositions from different fields in MgO-Cr_2O_3 plots (Fig. 3A–D) are due to different conditions during proto-kimberlite metasomatism of the lithospheric mantle, reflecting the different compositions of the lithospheric mantle beneath these fields.

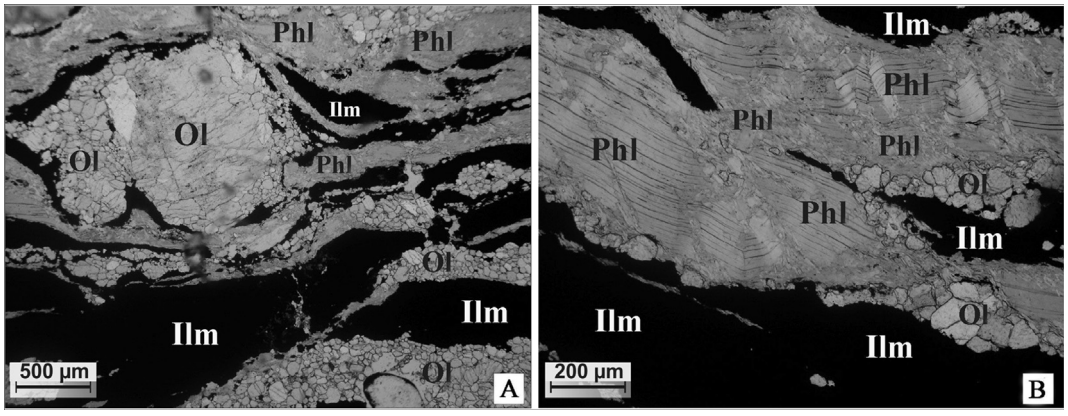

Fig. 11. Photomicrograph of Sample 00-83, a phl-ilm-ol sheared peridotite from the Udachnaya-East pipe. Note: Ilm forms veins and lenses.

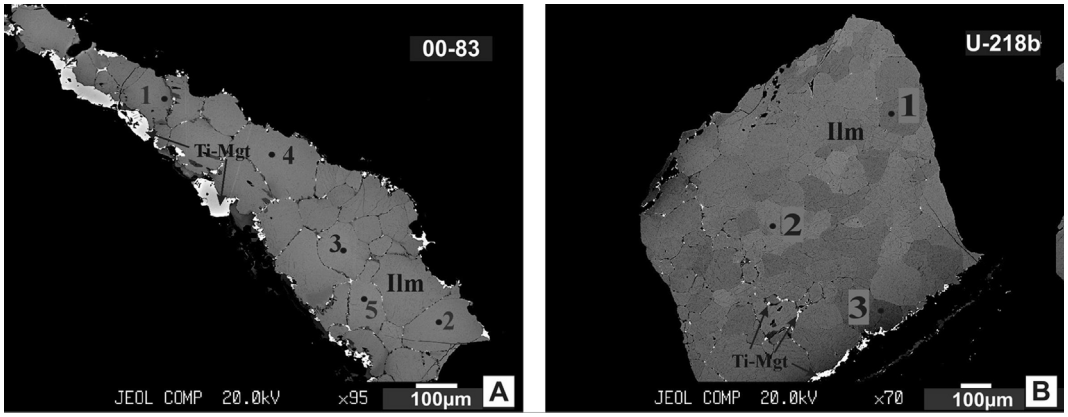

Fig. 12. Back-scattered electron images of ilmenite (ilm) grains with a polygranular texture from samples: 00-83 (A) and U-218b (B). The size of the granules is 20–250 μm. Titaniferous-magnetite is located in the interstices between the ilm granules and at the boundaries of the ilm lenses.

5.2. An asthenospheric source for kimberlites, and their megacryst suite

Radiogenic isotope systematics (Nowell et al., 2004; Woodhead et al., 2009; Tappe et al., 2012), the Mg#, Cr, and Ni contents of kimberlite melts (e.g., Price et al., 2000; Soltys et al., 2018), sub-lithospheric xenoliths (Sautter et al., 1991; Haggerty, 2017), as well as deeply derived diamonds (Stachel, 2001; Harte, 2010; Kaminsky, 2012; Pearson et al., 2014) in kimberlites globally suggest that the source of kimberlites occurs in the asthenosphere (Boyd and Nixon, 1975; Pasteris, 1979; Pearson et al., 1995).

A genetic link between kimberlites and the megacryst suite is indicated by their similar Rb-Sr, Sm-Nd, and Lu-Hf isotope systematics (Nowell et al., 2004; Kopylova et al., 2009; Kamenetsky et al., 2014). For example, initial $^{87}Sr/^{86}Sr$ values for the low-Cr megacryst suite as well as whole-rock kimberlites (Nowell et al., 2004; Becker and Le Roex, 2006) overlap the $^{87}Sr/^{86}Sr_{(i)}$ values of early crystallising kimberlite phases (i.e., perovskite and apatite – Malarkey et al., 2009; Paton et al. 2007; Woodhead et al., 2009).

The composition of primitive kimberlite melts are still the subject of debate. Estimates range from carbonatitic (e.g., Dawson and Hawthorne, 1973; Kamenetsky et al., 2008, 2014; Russell et al., 2012), to transitional silicate-carbonate (e.g., Brooker et al., 2011; Nielsen and Sand, 2008; Soltys et al., 2018), to volatile-rich ultramafic silicate melts (e.g., Kopylova et al., 2007; le Roex et al., 2003; Price et al., 2000). Likewise, the composition of the melt parental to the megacryst suite is equally controversial, where picritic (Harte, 1983), alkali-basaltic (Jones, 1987; Bruin, 1993De Bruin, 1993), or melts broadly similar to OIB (Nowell and Pearson, 1998) have been suggested. It was noted by Moore (2008) that REE modeling using partition coeffecitions for basaltic melt compositions argues against megacryst crystallization from the host kimberlite magma. However, the petrographic evidences provides strong evidence for genetic link between kimberlites and their megacryst suite, and suggests that megacrysts formed in the presence of carbonate-rich kimberlite liquids (Moore and Belousova, 2005). On the other hand, a genetic connection between kimberlites and alkaline basalts has been suggested based on their spatial and temporal relationships in the YKP (Rothman, 2002; Kiselev et al, 2009; Egorov et al., 2011) and other kimberlite provinces worldwide (Alibert et al., 1983; Araujo et al., 2001; Bizzi et al., 1993; Bogatikov et al., 1999).

5.3. Ilmenite in the kimberlite groundmass

Groundmass ilmenite occurs as anhedral to subhedral grains < 0.2 mm in size and has the highest MgO contents of any generation discussed here (up to 24 wt% - Danchin et al., 1975; Boctor & Boyd, 1980; Pasteris, 1980; Agee et al., 1982; Shee, 1984; Garanin et al., 1984, 1986). We interpret the composition of this ilmenite to represent evolution of the late stage kimberlite melt toward high MgO contents (see also Soltys et al., 2018b; Giuliani et al., 2017). Such Mg enrichment is also evidenced by zoned groundmass olivine (Sobolev et al., 2015; Brett et al., 2009).

Atypical groundmass ilmenite occurs in the Internatsional'naya pipe from the Mirninsky field (Fig. 13), where it forms acicular grains (from 100 × 10 to 350 × 30 μm in size). These groundmass ilmenite grains are enriched in MgO (up to 24 wt%), MnO (up to 3 wt%), and Nb_2O_3 (up to 6 wt%) compared to macrocrysts or megacrysts (Table 3).Fig. 14.

5.4. A xenocrystic or antecrystic origin of ilmenite macrocrysts?

The extreme rarity of ilm-bearing xenoliths compared with the high abundance of ilmenite macrocrysts in kimberlites of the Yakutian province argues against a strictly xenocrystic origin of these macrocrysts.

Table 3
Chemical composition of Ilm from the deformed peridotites of the Udachnaya-Eastern pipe and groundmass needle-like Ilm from Internatsionalnaya pipe (see Figs. 12, 13).

Samples	00–83 (Fig. 12A)					U-218b (Fig. 12B)			00–287 (Fig. 13)	
Points	1	2	3	4	5	1	2	3	13A-3	13B-12
TiO_2	47.57	45.83	45.67	45.14	45.39	50.07	49.95	50.01	52.64	50.45
Al_2O_3	0.59	0.6	0.46	0.85	0.35	0.63	0.46	0.37	0.03	0.06
Cr_2O_3	2.94	2.82	2.63	2.75	2.74	0.28	0.32	0.38	0.04	0.08
FeO	34.79	40.5	40.93	40.78	42.58	37.92	38.43	37.31	10.22	10.65
MnO	0.48	0.25	0.21	0.17	0.23	0.17	0.16	0.23	3.75	4.31
MgO	12.95	9.81	10.16	9.55	8.59	10.78	10.62	11.74	25.64	23.03
Nb_2O_5	0.44	0.4	0.36	0.29	0.31	0.16	0.13	0.12	7.25	7.02
NiO	0.06	0.15	0.14	0.12	0.15	0.08	0.11	0.07	0.01	0.01
Total	99.82	100.36	100.56	99.65	100.34	100.09	100.18	100.23	99.58	95.61

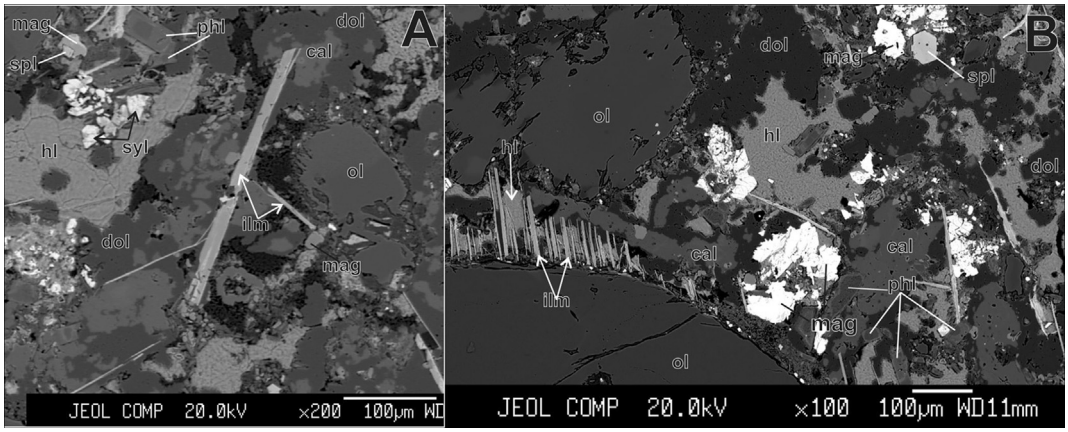

Fig. 13. Back-scattered electron images of acicular groundmass ilm from a serpentine-free kimberlite sample (№ 00–287) of Internatsional'naya pipe (see Table 3). Late stage groundmass ilm is overgrown by, and included in the dolomite-calcite-halite matrix, and may neucleate from olivine grain magrins.

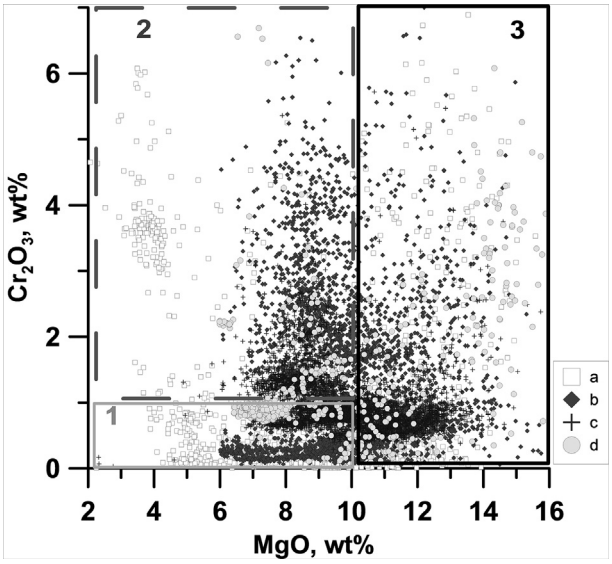

Fig. 14. MgO-Cr_2O_3 plot of ilm macrocrysts from all studied kimberlite fields with schematic designation of ilm crystallization stages (1, 2, and 3) as discussed in the main text. Kimberlite fields are labeled as follows: a - Mirninsky; b - Daldynsky; c - Alakit-Marhinsky; d - Verhnemunsky.

Compositional distributions of ilmenite megacrysts and ilmenite from mantle xenoliths in the Udachnaya-East kimberlite indicate subtle compositional differences (Fig. 2). The composition of ilmenite macrocrysts are grouped into three distinct tightly clustered groups in MgO-Cr_2O_3 space. In contrast, ilmenite from sheared peridotites forms two largely scattered fields. Ilmenite in sheared peridotites is characterized by a higher MgO and Cr_2O_3 contents. Therefore, a xenolithic source for many macrocrysts appears unlikely. On the other hand, the textural features of ilm-bearing sheared peridotites from the Udachnaya-East kimberlite (section 2.4) are similar to those of polygranular ilmenite nodules from the Mir pipe. The similarity of ilmenite deformation textures in sheared peridotites and polygranular nodules indicates their crystallization occurred prior to interaction with the (proto-)kimberlite fluids which caused deformation and eventual entrainment into the host kimberlite melt (Pasteris, 1979; Kostrovitsky et al., 2013). This scenario is consistent with the long ascent of kimberlite melts to the earth's surface, where these nodules may undergo recrystallization and change their compositions (e.g., Arndt et al., 2010).

The REE's compositions and distributions of garnets in sheared lherzolites and garnet megacrysts from the Udachnaya kimberlite (Kostrovitsky et al., 2004, 2008, 2013; Solov'eva et al., 2008) and other kimberlites worldwide (Moore & Lock, 2001) are similar, indicating a genetic relationship. Veins of ilmenite in sheared lherzolites further supports a genetic relationship between ilmenite macrocrysts and ilm-bearing sheared peridotites.

We suggest that stress at the lithosphere-asthenosphere boundary led to asthenospheric melt-fluid mobilization and ascent through the lithospheric mantle causing metasomatism and deformation of lherzolites (Boyd et al., 1997; Burgess and Harte, 2004). Immiscibility of an ilm-bearing fluid formed lenses and veins at deep lithosphere levels, which become the source for some proportion of ilmenite megacrysts/macrocrysts (Ashchepkov et al., 2014).

This model for the formation of kimberlitic ilmenite makes the question of whether ilmenite macrocrysts are xenocrystic redundant. The main conclusion is that the source of ilmenite was an asthenospheric (proto-kimberlitic?) melt and therefore ilmenite crystallization was connected with formation of kimberlites.

5.5. P-T conditions of ilmenite crystallization

Members of the Cr-poor megacryst suite crystallize over a wide temperature range 1410–1130 °C and at < 45 kb (Gurney et al., 1979; Moore et al., 1992, 2001). Ilmenite is suggested to have crystallised after garnet and orthopyroxene megacrysts, at the lower end of this wide temperature range. Megacrystic clinopyroxene is syngenetic with ilm, and is commonly used to evaluate the P-T parameters of ilmenite crystallization. Similar P-T parameters (i.e., 50 kb and 1165–1390 °C) were obtained by Agee et al. (1982) for crystallization of ilmenite megacrysts and ilm-cpx intergrowths from the kimberlites of Elliott Country, Kentucky. Slightly lower crystallization temperatures (i.e., 1025–1125 °C) of cpx megacrysts, which were presumably syngenetic with ilm, were obtained by Eggler et al. (1979) for kimberlites of the Sloan-Nix, Colorado-Wyoming kimberlites.

P-T crystallization parameters were calculated for ilmenite from the Udachnaya-East kimberlite from a locality with an unusually high concentration of ilmenite macrocrysts (i.e., ~40–50% of the whole rock – Kostrovitsky et al., 2004). This locality contains ilmenite nodules with inclusions of cpx, ilm-cpx intergrowths, as well as cpx and ol megacrysts. The P-T conditions of ilmenite crystallisation (i.e., 1054–1091 °C and 39.8–42.5 kb after Kostrovitsky et al, 2004) were obtained using the single clinopyroxene thermobarometer of Nimis & Taylor, (2000). Sr-Nd-Hf isotopic systematics were determined for a cpx megacryst (№ UV-9774) collected from this same ilm-rich locality (Kamenetsky et al., 2009). The isotopic composition of this megacryst ($(^{87}Sr/^{86}Sr)_i$ = 0.70292, εNd = +5.0, εHf = +6.5) overlaps those of perovskites from this kimberlite (Kamenetsky et al., 2009; Sun et al., 2014). We suggest that ilmenite megacrysts crystallised within the lithospheric mantle, at depths of ~140 km. Higher P-T conditions (i.e.,

1054–1150 °C and 6 GPa) were obtained for cpx-ol-ilmenite sheared peridotites from the Udachnaya-East pipe (Solov'eva et al., 2019), which corresponds to the approximate depth of the LAB beneath this cluster.

5.6. The presence and formation of ilmenite/oxide melts

The large size of ilmenite megacrysts (up to 4 cm), abundance of ilmenite in some kimberlites (e.g., up to 3 vol% – Oval pipe, Daldynsky field; Olymp pipe, Chomurdakh field), and ilmenite veins in sheared lherzolites (Fig. 11), whose origin can be linked to the Cr-poor megacryst suite, all indicate the existence of an ilmenite/oxide melt. The presence of metal oxide melts which crystallise ilmenite has been invoked by a number of researchers (e.g., Clarke and Mackay, 1990; Hong-Fu et al., 2001; Zhang et al., 2001; Wyatt et al., 2004; Kostrovitsky et al., 2004).

The presence of ilmenite veinlets in sheared lherzolites (Fig. 11) is evidence of the formation of such melts at depths which correspond to the asthenosphere-lithosphere boundary. Ilmenite liquation from the parental high-Ti asthenospheric melt was caused by a change in P-T conditions after deformation processes at the LAB. We assume that the latter initiated the formation of deformed lherzolites, and the ascent of the asthenospheric melt. Based on the widespread occurrence of sheared xenoliths and megacryst suit minerals in kimberlites worldwide it appears that such proto-kimberlite metasomatism of the lithosphere is a prequsite for successful kimberlite ascent to the surface. Ilmenite crystallization from the kimberlite melt continued to the later stages of ascent and possibly during and after kimberlite emplacement into the upper crust, as indicated by the presence of small groundmass ilmenite (Pasteris, 1980; Agee et al., 1982; Shee, 1984; Garanin et al., 1984, 1986).

5.7. Ilmenite and the diamond potential of kimberlites

Ilmenite is one of the main kimberlite indicator minerals (Haggerty, 1991a, 1991b; Mitchell, 1986; Wyatt et al., 2004) and has been utilized heavily in diamond exploration (Nixon et al., 1963; Boctor and Boyd, 1980; Haggerty and Tompkins, 1984; Mitchell, 1986; Griffin and Ryan, 1995; Gurney et al., 1993; Hood and McCandless, 2004; Kjarsgaard et al., 2004; Masum et al., 2004; Kostrovitsky et al., 2004, 2006; Van Straaten et al. 2008). The interpretation of ilmenite major element compositions used in diamond exploration has proven ineffective for identifying diamondiferous kimberlites (Gurney and Zweistra, 1995; Wyatt et al., 2004; Schulze et al. 1995; Robles-Cruz et al. 2009). For instance, late-stage Mg enrichment of ilmenite xenocrysts is unrelated to reducing conditions which favor diamond preservation within the mantle (Castillo-Oliver et al., 2017). The absence of a correlation between the diamond content of the host kimberlite and the Fe_2O_3 content of its ilmenite has been described for North American occurrences (Schulze et al., 1995), and the Catoca intrusions (Angola – Robles-Cruz et al., 2009).

Different mantle source regions for most diamonds (i.e., lithospheric) and macrocrystic ilmenite (i.e., asthenospheric), as well as their different origins (i.e., xenocrystic and antecrystic, respectively) underpin the lack of correlation between the abundance and composition of these minerals. The most diamondiferous pipes in the YKP – Aykhal (Alakit-Markhinsky field), Internatsional'naya and XXIII KPSS (Mirninsky field), Botuobinskaya and Nyurbinskaya (Nakynsky field, see Fig. 5s) are high-Mg kimberlites where ilmenite macrocrysts are either rare or non-existent (Kostrovitsky et al., 2015). On the other hand, there are large highly diamondiferous pipes (e.g., Mir, Zarnitsa, Yubileinaya, Udachnaya) which are Mg-Fe kimberlites and contain variable amounts of ilm. The maximum concentration of the hematite end-member in ilmenite is found in kimberlites of the Mirninsky field, which are characterized by different diamond grades, from high grade (Internatsional'naya pipe) to low grade (Taezhnaya pipe) (Figure Supplementary Fig. 10s).

6. Conclusions

A representative collection of ilmenite macrocrysts from the major diamondiferous kimberlite fields of the YKP was employed to propose a genetic association between ilmenite and kimberlite magmatism.

Different ilmenite compositional distributions were identified in MgO *vs*. Cr_2O_3 plots, and different distributions (i.e., Haggerty's parabola, step-like distributions) are dominate in particular kimberlite fields. The "Haggerty's parabola" distribution is typical of ilmenite from the Mirninsky field; the "step-like" distribution is typical of ilmenite from the Daldynsky field; the Verkhnemunsky field is dominated by a diffuse cluster of analysis and no clear evolutionary trend in MgO-Cr_2O_3 space; and a combination of the "Haggerty's parabola", "step-like" and "diffuse" distributions are observed in ilmenite from the Alakit-Markhinsky field.

Based on ilmenite macrocryst compositional distributions, the study of heterogeneity in polygranular ilmenite nodules, and ilmenite in sheared xenoliths, we propose a three stage formation and (re-)crystallization history of ilmenite macrocrysts and megacrysts: 1) primitive asthenospheric melt; 2) lithospheric contaminated melt and 3) re-equilibration with the host kimberlite during ascent through the lithosphere-crust.

The initial stage of ilmenite crystallization occurred in an asthenospheric melt with other megacrystic minerals of the Cr-poor suite. In accordance with previous studies, we suggest the primary mechanism for changing the composition of ilmenite (i.e., decreasing Mg, Cr, increasing Fe, Al concentrations), as well as other minerals of Cr-poor megacryst suite, was fractional crystallization.

The second stage of ilmenite crystallization is inferred to have occurred within the lithosphere. This ilmenite displays an increase in MgO and Cr_2O_3 contents, which reflects changes in the composition of the kimberlite melt during assimilation of lithospheric mantle material, forming the right branch of Hagerty's parabola in MgO *vs*. Cr_2O_3 bivariate plots.

The third stage of ilmenite re-crystallization (and re-equilibration) is recorded by the heterogeneity of individual grains. We propose recrystalisation of ilmenite under increasing fO_2 of the evolving kimberlite melt during ascent through the lithosphere (potentially continuing in the crust) caused the decreasing Fe and Mn contents, with corresponding increases in Mg content, yet Cr contents of remain unchanged. In our view, this process explains the production of the right branch of "Haggerty's parabola". We note that these three ilmenite (re-)crystallization stages were realized in different clusters (i.e., different conduits) to varying degrees.

The formation of other ilmenite compositional distribution patterns (e.g., "step-wise", and "hockey stick") is attributed to different compositions of the entrained and partially assimilated lithospheric mantle material, and different ascent dynamics in each of the different kimberlite conduits (which were different for each different kimberlite cluster).

All kimberlite pipes of the same cluster are characterized by similar ilmenite compositions and the same compositional distribution, whereas ilmenite from different clusters have distinct average compositions and compositional distributions (Kostrovitsky et al, 2003; Kostrovitsky, 2017). Similar ilmenite compositional distributions are also typical of other kimberlite provinces worldwide, and we infer similar process to be responsible for these compositional distributions in kimberlitic ilmenite globally (e.g., Haggerty, 1975; Shee and Gurney, 1979; Eggler et al., 1979; Schulze, 1984; Mitchell, 1986; Moore et al., 1992; Wyatt et al., 2004; Robles-Cruz et al., 2009). These compositional features are attributed to the existence of a single magmatic conduit feeding all pipes of a given cluster, and different conduits feeding different clusters. Proto-kimberlite melt compositions evolved separately in each cluster (conduit) by the incorporation and partial assimilation

of distinct lithospheric mantle material, leading to distinct ilmenite composition in each kimberlite cluster.

The presence of large ilmenite megacrysts (up to 7 cm in size), the abundance of ilmenite macrocrysts and megacrysts (up to 1–3 vol%) in some kimberlites, and ilmenite veins in sheared peridotites suggest ilmenite crystallisation following immiscibility of a oxide-carbonate-silicate melt (see also Clarke & Mackay, 1990; Zhang et al., 2001; Kostrovitsky et al., 2004; Giuliani et al., 2014). We suggest that the process of immiscibility (liquation) of the proto-kimberlite melt occurred as a result of stresses at the asthenosphere – lithosphere boundary.

Therefore, although ilmenite is a part of Cr-poor megacryst suite, its crystallization was not limited to the asthenosphere, but continued during proto-kimberlite metasomatism of the lithosphere, and continued to (re-)crystallise and re-equilibrate with the host kimberlite melt during ascent through the lithosphere, and possibly continuing after emplacement in the upper crust. These findings are consistent with (proto-)kimberlite magmatism occurring for an extended period (i.e., ~5 Ma) before eventual emplacement of the host kimberlite into the upper crust (e.g., Moore, 2008).

If correct, the duration of kimberlite ascent was not as short as described in a number of publications (i.e., 4–20 m/s with eruption durations of many hours to months – e.g., Sparks et al., 2006; Wilson and Head, 2007). At least, this time was sufficient for the assimilation lithospheric material and (re-)crystallization of deep-seated minerals.

Declaration of Competing Interest

The authors declare that they have no known competing financial interests or personal relationships that could have appeared to influence the work reported in this paper.

Acknowledgments

The authors thank the geological management of AK ALROSA for creating favorable conditions during the field work, for financial assistance. The study was carried out within the framework of the state task on Project IX.129.1.5. (No. 0350-2016-0030). The study was carried out using the equipment of the Centre of collective usage “Isotope-geochemical research” of Institute of Geochemistry, Siberian branch of Russian Academy of Sciences.

Appendix A. Supplementary data

Supplementary data to this article can be found online at https://doi.org/10.1016/j.oregeorev.2020.103419.

References

Agashev, A.M., Pokhilenko, N., Tolstov, Alexandr, Polyanichko, V., Malkovets, Vladimir, Sobolev, N., 2004. New age data on kimberlites from the Yakutian diamondiferous province. Doklady Earth Sci. 399, 1142–1145.

Agee, J.J., Garrison Ir, J.R., Taylor, L.A., 1982. Petrogenesis of oxide minerals in kimberlite, Elliot County. Kentucky. Amer. Mineral. 67, 28–42.

Alibert, C., Michard, A., Albarede, F., 1983. The transition from alkali basalts to kimberlites: isotope and trace element evidence from melilitites. Contrib. Mineral. Petrol. 82, 176–186.

Araujo, A.L.N., Carlson, R.W., Gaspar, J.C., Bizzi, L.A., 2001. Petrology of kamafugites and kimberlites from the Alto Paranaiba alkaline province, Minas Gerais, Brazil. Contrib. Mineral. Petrol. 142, 163–177.

Ashchepkov, I.V., Alymova, N.V., Logvinova, A.M., Vladykin, N.V., Kuligin, S.S., Mityukhin, S.I., Downes, H., Stegnitsky, Yu.B., Prokopiev, S.A., Salikhov, R.F., Palessky, V.S., Khmel'nikova, O.S., 2014. Picroilmenites in Yakutian kimberlites: variations and genetic models. Solid Earth 5, 915–938. https://doi.org/10.5194/se-5-915-2014.

Alymova, N.V., Kostrovitsky, S.I., Ivanov, A.S., Serov, V.P., 2004. Picrolmenite from kimberlites of the Daldyn field (Yakutia). Doklady of the Russian Academy of Sciences. 395 (6), 799–802 (in Russian).

Amshinsky, A.N., Pokhilenko, N.P., 1983. The features of composition Ilmenite from Zarnitsa pipe. Russian Geol. Geophys. 11, 116–119 (in Russian).

Arndt, N.T., Guitreau, M., Boullier, A.M., le Roex, A., Tommasi, A., Cordier, P., Sobolev, A., 2010. Olivine, and the origin kimberlite. J. Petrol. 51 (3), 573–602.

Bogatikov, O.A., Kononova, V.A., Golubeva, Y.Y., Zinchuk, N.N., Ilupin, I.P., Rotman, A.Y., Levsky, L.K., Ovchinnikova, G.V., Kondrashov, I.A., 2004. Variations in chemical and isotopic compositions of the Yakutian kimberlites and their causes. Geochem. Int. 42, 799–821.

Baptiste Virginie, Tommasi Andréa; Demouchy Sylvie. 2012. Deformation and hydration of the lithospheric mantle beneath the Kaapvaal craton, South Africa. LITHOS, Volume 149, p. 31-50.

Bizzi L.A., Smith C.B., De Wit M.J., Armstrong R.A., Meyer H.O.A., 1993. Mesozoic kimberlites and related alkaline rocks in southwestern Sao Francisco craton: a case for local mantle reservoirs and their interaction. Araxa Proceedings of 5th IKC. P. 156-171.

Blagul'kina, V.A., Gubanov, V.A., Umanen, V.N., Futergendler, S.I., 1975. Microcrystals of ilmenite from kimberlites of Luchakan Area. In book.: Minerals and parageneses of minerals of endogenous deposits. Nauka, Leningrad, pp. 11–18 (in Russian).

Boctor N.Z., Meyer H.J.A., 1979. Oxide and sulfide minerals in kimberlite from Green Mountain, Colorado. Proceedings of 2-nd IKC. V. 1. P. 217-228.

Boctor, N.Z., Boyd, F.R., 1977. Oxide minerals in the Liqhobong kimberlite, Lesotho. Annual Report the Director Geophysical Laboratory Carnegie Institution. 870–876.

Boctor, N.Z., Boyd, F.R., 1980. Oxide minerals in the Liqhobong kimberlite. Lesotho. Amer. Mineral. 65, 631–638.

Bogatikov O.A., Garanin V.K., Kononova V.A., Kudryavtseva G.P., Vasileva E.P., Verzhak V.V., Verichev E.M., Posuhova T.V., 1999. Arkhangelsk diamond province (geology, petrography, geochemistry and mineralogy) Moscow Univ. Press. 524 p. (In Russian).

Boyd F.R., Nixon P.H., 1975. Origin of the ultramafic nodules from some kimberlites of Northern Lesotho and the Monastery Mine, South Africa. In: Physics and Chemistry of the Earth. New York: Pergamon Press. V. 9. P. 431-454.

Boyd, F.R., Pokhilenko, N.P., Pearson, D.G., Mertzman, S.A., Sobolev, N.V., Finger, L.W., 1997. Composition of Siberian cratonic mantle: evidence from Udachnaya xenoliths. Contrib. Miner. Petrol. 128, 228–246.

Brett, R.C., Russell, J.K., Moss, S., 2009. Origin of olivine in kimberlite: phenocryst or imposter? Lithos 112, 201–212.

Burgess, S.R., Harte, B., 2004. Tracing lithosphere evolution through the analysis of heterogeneous G9/G10 garnet in peridotite xenoliths, II: REE Chemistry. J. Petrol. 45, 609–634.

Clarke, D.B., Mackay, R.M., 1990. Ilmenite-garnet-clinopyroxene nodule from Matsoku. Evidence for oxide-rich liquid immiscibility in kimberlites. Can. Mineral. 28 (pt 2), 229–239.

Castillo-Oliver, M., Melgarejo, J.C., Galí, S., Pervov, V., Gonçalves, A.O., Griffin, W.L., Pearson, N.J., O'Reilly, S.Y., 2017. Use and misuse of Mg- and Mn-rich ilmenite in diamond exploration: a petrographic and trace element approach. Lithos 292–293, 348–363.

Danchin, R.W., Ferguson, J., Mclver, J.R., Nixon, P.H., 1975. The composition of late-stage kimberlite liquidsas revealedby nucleated autoliths. Phys. Chem, Earth. 9, 235–245.

Davis, B.T.C., Boyd, F.R., 1966. The join $Mg_2Si_2O_6$-$CaMgSi_2O_6$ at 30 kbar pressure and its applicationto pyroxenes from kimberlites. J. Geophysical Res. 71, 3567–3576.

De Bruin, D., 1993. The megacryst suite from the Schuller kimberlite, South Africa. Bull. Geol. Survey of South Africa 114, 112 pp.

Bruin, De, 2005. Multiple compositional megacryst groups from the Uintjiesberg and Witberg kimberlites, South Africa. S. Afr. J. Geol. 108, 233–246.

Eggler D.H., McCallum M.E., Smith C.B., 1979. Megacrysts assemblages in kimberlite from Northern Colorado and South Wyoming. In: The Mantle Sample: inclusions in kimberlites and other volcanics. 2 Int. kimberlite conf. V. 2. P. 213-226.

Eggler, D.H., 1983. Upper mantle oxidation state: Evidence from olivine-orthopyroxene-ilmenite.assemblages. Geophys. Res. Lett. 10, P.365-368.

Egorov, K.N., Kiselev, A.I., Yarmolyuk, V.V., Nikiforov, A.V., 2011. Composition and sources of magmatism of the Middle Paleozoic Vilyui rift region and the problem of combining its basal and kimberlite derivatives. DAN. 436 (2), 221–227 (in Russian).

Elthon D., Ridley W.I., 1979. The oxide and silicate mineral chemistry of a kimberlite from the Premier Mine: Implications for the evolution of kimberlitic magmas. In: Proceedings of 2-nd IKC. V. 1. P. 206-216.

Frantsesson E.V. 1968. Petrology of kimberlites. M.: Nedra. 200 p. (in Russian).

Frick, C., 1973. Kimberlitic ilmenites. Trans. Geol. Soc., South Africa. 76, 195–200.

Garanin, V.K., Kudryavtseva, G.P., 1979. Some dependence “composition-structure-features” for ilmenite from Yakutian kimberlites and their mineralogical value. Zapiski VMO. 108 (1), 38–47 (in Russian).

Garanin, V.K., Kudryavtseva, G.P., Soshkina, L.T., 1984. Ilmenite from kimberlites. M.: Publishing House of the Moscow State. University. 240, p (in Russian).

Garanin V.K., Kudryavtseva G.P., Mihailichenko O.A., 1986. Mineralogy of ilmenite from kimberlite groundmass. Materials of the 8th conference of young scientists “Mineralogy of kimberlites and related rocks”. VINITI, Moscow. P. 184-207. (in Russian).

Giuliani, A., Kamenetsky, V.S., Kendrick, M.A., Phillips, D., Wyatt, B.A., Maas, R., 2013. Oxide, sulphide and carbonate minerals in a mantle polymict breccia: Metasomatism by proto-kimberlite magmas, and relationship to the kimberlite megacrystic suite. Chem. Geol. 353, 4–18.

Giuliani, A., et al., 2014a. Stable isotope (C, O, S) compositions of volatile-rich minerals in kimberlites: a review. Chem. Geol. 374–375, 61–83.

Giuliani, A., et al., 2014b. Petrogenesis of mantle polymict breccias: insights into mantle processes coeval with kimberlite magmatism. J. Petrol. 55 (4), 831–858.

Green, D.H., Sobolev, N.V., 1975. Coexisting garnets and ilmenites synthesized at high pressures from pyrolite and olivine basanite and their significance for kimberlitic assemblages. Contrib. Mineral. Petrol. 50, 217–229.

Griffin, W.L., Moore, R.O., Ryan, C.G., Gurney, J.J., Win, T.T., 1997. Geochemistry of magnesian ilmenite megacrysts from Southern African kimberlites. Russ. Geol.

Geophys. 38 (2), 398–419.
Griffin, W.L., Ryan, C.G., 1995. Trace elements in indicator minerals: area selection and target evaluation in diamond exploration. J. Geochem. Explor. 53, 311–337. https://doi.org/10.1016/0375-6742(94)00015-4.
Gurney, J.J., Helmstaedt, H., Moore, R.O., 1993. A review of the use and application of mantle mineral geochemistry in diamond exploration. Pure Appl. Chem. 65 (12), 2423–2442.
Gurney, J.J., Zweistra, P., 1995a. The interpretation of the major element compositions of mantle minerals in diamond exploration. J. Geochem. Explor. 53, 293–309. https://doi.org/10.1016/0375-6742(94)00021-3.
Gurney J.J., Jacob W.R.O., Dawson J.B., 1979. Megacrysts from the Monastery kimberlite pipe. In: F.R. Boyd, Y.O.A. Meyer. (Editors). The mantle sample: inclusions in kimberlites and other volcanics. Am.Geophys. Union. Washington. (Proceedings of 2-nd IKC). P. 227-243.
Gurney, J.J., Zweistra, P., 1995b. The interpretation of major element compositions of mantle minerals in diamond exploration. J. Geochem. Explor. 53, 293–309.
Haggerty, S.E., 1975. The chemistry and genesis of opaque minerals in kimberlite. Phys. Chem. Earth. New York. 9, 227–243.
Haggerty S.E., Hardie R.B., McMahon B.M., 1979. The mineral chemistry of ilmenite nodule associations from the Monastery diatreme. In the book: The mantle samples: inclusions in kimberlites and other volcanics. P. 249-256.
Haggerty, S.E., Tompkins, L.A., 1984. Subsolidus reactions in kimberlitic ilmenites: exsolution, reduction and the redox state of the mantle, in Kimberlites I. Proc. Kimberlite Conf. 1, 335–357.
Haggerty S.E. 1991a. Oxide mineralogy of the upper mantle. In:Lindsley DH, Ribbe HP (eds) Oxide minerals: petrological and magnetic significance. (Reviews in Mineralogy, 25) Mineral Soc Am, Washington, DC, pp 355-416.
Haggerty S. E. 1991b, Oxide textures: A mini-atlas, in Oxide Minerals: Petrologic and Magnetic Significance, Rev. Mineral., vol. 25, edited by D. H. Lindsley, pp. 129 – 137, Mineral. Soc. of Am., Washington, D. C.
Haggerty, S.E., 2016. Kimberlite discoveries in NW Liberia: tropical exploration & preliminary results. J. Geochem. Explor. 173, 99–109.
Harte, B., 1977. Rock nomenclature with particular relation to determination and recrystallization textures in olivine-bearing xenoliths. J. Geol. 85, 279–288.
Harte, B., Gurney, J.J., 1981. The mode of formation of chromium-poor megacryst suites from kimberlites. J. Geol. 89, 749–753.
Harte, B., 1983. Mantle peridotites and processes – the kimberlite sample. In: Hawkesworth, C.J., Norry, M.J. (Eds.), Continental basalts and mantle xenoliths. Shiva Publishing Limited, Cheshire, pp. 46–99.
Hood, C.T.S., McCandless, T.E., 2004. Systematic variations in xenocrysts mineral composition at the province scale. Buffalo Hills kimberlites, Alberta, Canada, Lithos 77, 733–747.
Ilupin, I.P., Milashev, V.A., Tomanovskaya, Yu.I., Evdokimov, A.N., 1974. Ilmenite from Yakutian kimberlite. In book: Mineralogy, Geochemistry and Forecasting of Diamond Deposits. Leningrad: NIIGA. P. 5-29. (in Russian).
Ilupin, I.P., Kaminsky, F.V., Frantseson, E.V., 1978. Geochemistry of kimberlites. Moskow: Nedra. 352p. (in Russian).
Jones, R.A. Sr and Nd isotopic and rare earth element evidence for the genesis of megacrysts in kimberlites of southern Africa. In: Mantle xenoliths, edit. by P.H.Nixon, John Wiley & Sons Ltd. 1987. P. 711-724.
Jones, A.P., Wyllie, P.J., 1984. Minor elements in perovskite from kimberlites and the distribution of rare earth elements: An electron probe study. Earth Planet. Sci. Lett. 69, 128–140.
Kamenetsky, V.S., Kamenetsky, M.B., Sobolev, A.V., Golovin, A.V., Demouchy, S., Faure, K., Sharygin, V.V., Kuzmin, D.V., 2008. Olivine in the Udachnaya-East kimberlite (Yakutia, Russia): types, compositions and origins. J. Petrol. 49, 823–839.
Kamenetsky, V.S., Maas, R., Kamenetsky, M.B., Paton, C., Phillips, D., Golovin, A.V., Gornova, M.A., 2009. Chlorine from the mantle: magmatic halides in the Udachnaya-East kimberlite, Siberia. Earth Planetary Sci. Lett. 285, 96–104.
Kamenetsky, V.S., Belousova, E.A., Giuliani, A., Kamenetsky, M.B., Goemann, K., Griffin, W.L., 2014. Chemical abrasion of zircon and ilmenite megacrysts in the Monastery kimberlite: Implications for the composition of kimberlite melts. Chem. Geol. 383, 76–85.
Kargin, A.V., Sazonova, L.V., Nosova, A.A., Pervov, V.A., Minevrina, E.V., Khvostikov, V.A., Burmii, Z.P., 2017. Sheared peridotite xenolith from the V. Grib kimberlite pipe, Arkhangelsk Diamond Province, Russia: Texture, composition, and origin. Geosci. Front. 8 (4), 653–669.
Kennedy, Lori, Russell, James, Kopylova, Maya, 2002. Mantle shear zones revisited: The connection between the cratons and mantle dynamics. Geology 30, 419–422.
Kinny, P.D., Griffin, B.J., Heaman, L.M., Brakhfogel, F.F., Spetsius, Z.V., 1997. SHRIMP U-Pb ages of perovskite from Yakutian kimberlites. Russ. Geol. Geophys. 38, 97–105.
Kiselev, A.I., Yarmolyuk, V.V., Egorov, K.N., 2009. Potassium basalts and picrobasalts from the Devonian kimberlite fields of Western Yakutia, Russia, and their relations to kimberlite magmatism. Geol. Ore Deposits 51 (1), 33–50 (in Russian).
Kononova, V.A., Golubeva, Yu.Yu., Bogatikov, O.A., 2005. Geochemical (ICP-MS geochemistry, isotopy of Sr, Nd, and Pb) heterogeneity of Yakutian kimberlites: problems of genesis and diamond potential. Petrologiya 13 (3), 227–252.
Kopylova, M.G., Russell, J.K., Cookenboo, H., 1999. Petrology of peridotite and pyroxenite xenoliths from the Jericho kimberlite: Inferences for the thermal state of the mantle beneath the Slave craton, northern Canada. J. Petrol. 40, 79–104.
Kopylova, M.G., Nowell, G.M., Pearson, D.G., Markovic, G., 2009. Crystallization of megacrysts from protokimberlitic fluids: geochemical evidence from high-Cr megacrysts in the Jericho kimberlite. Lithos 112S, 284–295.
Kostrovitsky, S.I., 1986. Geochemical features of minerals from kimberlites. Nauka, Novosibirsk 263p. (in Russian).
Kostrovitsky, S.I., Alymova, N.V., Ivanov, A.S., Serov, V.P., 2003. Structure of the Daldyn field (Yakutian province) on the base of study of picroilmenite composition. Abstracts on CD. 8 International Kimberlite Conference. 5p.
Kostrovitsky, S.I., Malkovets, V.G., Verichev, E.M., Garanin, V.K., Suvorova., L.V., 2004a. Megacrysts from the Grib kimberlite pipe (Arkhangelsk province, Russia). Lithos 77, 511–523.
Kostrovitsky, S.I., Spetsius, Z.V., Alymova, N.V., Suvorova, L.Ph., 2004b. Clinopyroxene-olivine-ilmenite megacryst association from kimberlites of Udachnaya pipe. Dokladi Russian academy of sciences. 396 (1), 93–97 (in Russian).
Kostrovitsky, S.I., Alymova, N.V., Yakovlev, D.A., Serov, I.V., Ivanov, A.S., Serov, V.P., 2006a. Features of chemical picroilmenite composition from diamond-bearing fields of the Yakutian Province. Doklady of Russian Academy of Sciences. 406 (3), 350–354 (in Russian).
Kostrovitsky, S.I., Alymova, N.V., Yakovlev, D.A., Serov, V.P., 2006b. Mineralogical Passports of the different taxons of kimberlite volcanism. Russian Journal: Ores and metals. No 4, 27–36 (in Russian).
Kostrovitsky, S.I., Morikiyo, T., Serov, I.V., Yakovlev, D.A., Amirzhanov, A.A., 2007. Isotope-geochemical systematics of kimberlites and related rocks from the Siberian Platform. Russ. Geol. Geophys. (1068-7971) 48 (3), 272–290. https://doi.org/10.1016/j.rgg.2007.02.011.
Kostrovitsky, S.I., Solov'eva, L.V., Gornova, M.A., Alymova, N.V., Yakovlev, D.A., 2008. About origin of megacrysts of garnet from kimberlites. Dokladi Russian Academy of Sciences 420 (2), 225–230 (in Russian).
Kostrovitsky, S.I., Spetsius, Z.V., Yakovlev, D.A., Fon der Flaass, G.S., Suvorova, L.Ph., Bogush, I.N., 2015. Atlas of the indigenous diamond deposits of the Yakut kimberlite province. Editor academician N.P. Pokhilenko. Mirny: Printing house of OOO "MGP". 480, p (in Russian).
Kostrovitsky, S., 2018. Deciphering kimberlite field structure using Mg-ilmenite composition: example of Daldyn field. (Yakutia). European Journal of Mineralogy. V. 30 No 6. https://doi.org/10.1127/ejm/2018/0030-2783.
Masum, K.M., Doyle, B.J., Ball, S., Walker, S., 2004. The geology and mineralogy of the Anuri kimberlite. Nunavut, Canada, Lithos 76, 75–96.
Milashev, V.A., 1965. Petrochemistry of Yakutian kimberlites and factors of their diamond potential. [in Russian]. Nedra, Leningrad.
Mitchell, R.H., 1973. Magnesian ilmenite and its role in kimberlite petrogenesis. J. Geol. 81, 301–311.
Mitchell, R.H., 1986. Kimberlites: mineralogy, geochemistry, and petrology. Plenum Press, New York, pp. 442.
Moore, A.E., 1987. A model for the origin of ilmenite in kimberlite and diamond: implications for the genesis of the discrete nodule (megacryst) suite. Contrib Mineral. Petrol. 95, 245–253.
Moore, R.O., Griffin, W.L., Gurney, J.J., Ryan, C.G., Cousens, D.R., Sie, S.H., Suter, G.F., 1992. Trace element geochemistry of ilmenite megacrysts from the Monastery kimberlite, South Africa. Lithos 29, 1–18.
Moore, R.O., Lock, N.P., 2001. The origin of mantle-derived megacrysts and sheared peridotites – evidence from kimberlites in the northern Lesotho. Orange Free State (South Africa) and Botswana pipe clusters. S. Afr. J. of Geol. 104, 23–38.
Moore, A., Belousova, E., 2005. Crystallization of Cr-poor and Cr-rich megacryst suites from the host kimberlite magma: implications for mantle structure and the generation of kimberlite magmas. Contrib. Mineral. Petrol. 149, 462–481.
Moore, A.E., 2008. Comments on the paper "Megacryst suites from the Lekkerfontein and Uintjiesberg kimberlites, southern Africa: evidence for a non-cognate origin". S. Afr. J. Geol. 111 (4), 462–464.
Nimis, P., Taylor, W., 2000. Single clinopyroxene thermobarometry for garnet peridotites. Part I. Calibration and testing of a Cr-in-Cpx barometer and an enstatite-in-Cpx thermometer. Contrib. Mineral. Petrol. 139, 541–554.
Nixon, P.H., von Knorring, O., Rooke, J., 1963. Kimberlites and associated inclusions of Basutoland: a mineralogical and geochemical study. Am. Mineral. 48, 1090–1132.
Nixon, P.H., Boyd, F.R., 1973. The discrete nodule (megacryst) association in kimberlites from northern Lesotho. In: Nixon, P.H. (Ed.), Lesotho kimberlites. Cape and Transvaal Printers, South Africa, pp. 67–75.
Nowell, G.M., Pearson, D.G., 1998. Hf isotope constrains on the genesis of kimberlitic megacrysts: evidence for a deep mantle component in kimberlites. Extended Abstracts of 7-th IKC. Cape Town, South Africa. 634–636.
Nowell, G.M., Pearson, D.G., Bell, D.R., Carlson, R.W., Smith, C.B., Noble, S.R., 2004. Hf isotope systematics of kimberlites and their megacrysts: new constraints on their source regions. J. Petrol. 45 (5), 1583–1612.
Nowicki, Thomas, Moore, Rory, Gurney, John, Baumgartner, Mike, 2007. Chapter 46 diamonds and associated heavy minerals in kimberlite: a review of key concepts and applications. Dev. Sedimentology 58, 1235–1267. https://doi.org/10.1016/S0070-4571(07)58046-5.
O'Reilly, Suzanne, Griffin, William, 2010. The continental lithosphere-asthenosphere boundary: Can we sample it? Lithos. 120.
Pasteris J.D., 1979. The ilmenite association at the Frank Smith Mine, R.S.A. Proceedings of 2-nd IKC. V. 2. P. 265-278.
Pasteris, J.D., 1980. The significance of groundmass ilmenite and megacryst ilmenite in kimberlites. Contrib. Mineral. Petrol. 75 (4), 315–325.
Pearson, D.G., Shirey, S.B., Carlson, R.W., Boyd, F.R., Pokhilenko, N.P., Shimizu, N., 1995. Re-Os, Sm-Nd, and Rb-Sr isotope evidence for the thick Archaean lithospheric mantle benith the Siberian craton modified by multistage metasomatism. Geochemica et Cosmochimica Acta. 59 (5), 959–977.
Rehfeldt, T., Jacob, D.E., Carlson, R.W., Foley, S.F., 2007. Fe-rich Dunite Xenoliths from South African Kimberlites: Cumulates from Karoo Flood Basalts. J. Petrol. 48 (7), 1387–1409.
Robles-Cruz, S.E., Watangua, M., Isidoro, L., Melgarejo, J.C., Galí, S., Olimpio, A., 2009. Contrasting compositions and textures of ilmenite in the Catoca kimberlite, Angola, and implications in exploration for diamond. Lithos 112S, 966–975.

Rodionov, A.S., Pokhilenko, N.P., Sobolev, N.V., 1984. Comparative study of the main minerals of concentrate of two kimberlite varieties, Dalnya pipe (Yakutia). Russian Geology and Geophysics. No 5, 38–49 (in Russian).
Rothman, A.J., 2002. Subalkaline basic rocks of kimberlite-controlling structures from eastern part of the Siberian platform. Ph.D. Thesis. Institute of Geology and Mineralogy. Russian), Novosibirsk, (In.
Russell, J.K., Porritt, L.A., Lavallee, Yan, Dingwell, D.B., 2012. Kimberlite ascent by assimilation – fuelled buoyancy. Nature 481 (19), 352–356.
Schulze D.J., 1984. Cr-poor megacrysts from the Hamilton Branch kimberlite, Elliot Country, Kentucky. Proceedings of 3-rd IKC. V. 2. Kimberlites II: The mantle and crust-mantle relationships. J. Kornprobst, ed. Elsevier Press, New York. P. 97-108.
Schulze, D.J., Anderson, P.F.N., Hearn, B.C., Hetman, C.M., 1995. Origin and significance of ilmenite megacrysts and macrocrysts from kimberlite. Int. Geol. Rev. 37, 780–812.
Scott Smith B.H, Nowicki T.E, Russell J.K, Webb K.J, Mitchell R.H, Hetman C.M, Harder M, Skinner E.M.W, Robey J.V. 2013. Kimberlite terminology and classification. Proceedings of the 10th International Kimberlite Conference. Special Issue J Geol Soc India, 2: P. 1–17. Springer India.
Shee S.R., Gurney J.J., 1979. The mineralogy of xenoliths from Orapa, Botswana. In: F.R. Boyd, Y.O.A. Meyer. (Editors). The mantle sample: inclusions in kimberlites and other volcanics. Am.Geophys. Union. Washington. (Proceedings of 2-nd IKC) P. 37-49.
Shee S.R., 1984. The oxides minerals of the Wesselton Mine kimberlite, Kimberly, South Africa. Proceedings of 3-rd IKC. V. 1. Kimberlites I: Kimberlates and Related Rocks. J. Kornprobst, ed. Elsevier Press, New York. P. 59-73.
Sobolev, N.V., 1974. Mantle Xenoliths in Kimberlites. Nauka, Novosibirsk 264, pp (in Russian).
Sobolev, N.V., Sobolev, A.V., Tomilenko, A.A., Kovyazin, S.V., Batanova, V.G., Kuz'min, D.V., 2015. Paragenesis and complex zoning of olivine macrocysts from unaltered kimberlite of the Udachnaya-east pipe (Yakutia): relationship with the kimberlite formation conditions and evolution. Russ. Geol. Geophys. 56, 260–279 (in Russian).
Solov'eva, L.V., Vladimirov, B.M., Dneprovskaya, L.V., Maslovska, M.N., Brandt, S.B., 1994. Kimberlites and related rocks. The substance of the upper mantle under the ancient platforms. Novosibirsk. Science 256, p (in Russian).
Solov'eva, L.V., Lavrent'ev, Yu.G., Egorov, K.N., Kostrovitsky, S.I., Korolyuk, V.N., Suvorova, L. Ph., 2008. Genetic connection sheared peridotites and garnet megacrysts from kimberlites and asthenosphere melts. Russ. Geol. Geophys. 49 (4), 281–301.
Solov'eva, L.V., Kalashnikova, T.V., Kostrovitsky, S.I., et al., 2017. Phlogopite and phlogopite–amphibole parageneses in the lithospheric mantle of the Birekte terrane (Siberian craton). Dokl. Earth Sc. 475, 822–827. https://doi.org/10.1134/S1028334X17070273.
Solov'eva L.V., Kostrovitsky S. I., Kalashnikova T.A., Ivanov A.V. 2019. The nature of phlogopite–ilmenite and ilmenite paragenesises in deep-seated xenoliths from Udachnaya kimberlite pipe. Dokladi in Russian academy of sciences. In press. (in Russian).
Soltys, Ashton, Giuliani, Andrea, Phillips, David, Kamenetsky, Vadim, Maas, Roland, Woodhead, Jon, Rodemann, Thomas, 2016. In-situ assimilation of mantle minerals by kimberlitic magmas — Direct evidence from a garnet wehrlite xenolith entrained in the Bultfontein kimberlite (Kimberley, South Africa). Lithos 256–257, 182–196. https://doi.org/10.1016/j.lithos.2016.04.011.
Soltys, Ashton, Giuliani, Andrea, Phillips, David, 2018a. A new approach to reconstructing the composition and evolution of kimberlite melts: A case study of the archetypal Bultfontein kimberlite (Kimberley, South Africa). Lithos 304–307, 1–15.
Soltys, Ashton, Giuliani, Andrea, Phillips, David, 2018b. Crystallisation sequence and magma evolution of the De Beers dyke (Kimberley, South Africa). Mineralogy and Petrology. V. 112. Supplement 2, 503–518.
Sparks, R.S.J., Baker, L., Brown, R.J., Field, M., Schumacher, J., Stripp, G., Walters, A., 2006. Dynamical constraints on kimberlite volcanism. J. Volcanol, and Geothermal Research 155, 18–48.
Stiefenhofer, Johann, Viljoen, K., Marsh, J., 1997. Petrology and geochemistry of peridotite xenoliths from the Letlhakane kimberlites. Botswana. Contributions to Mineralogy and Petrology. 127, 147–158. https://doi.org/10.1007/s004100050272.
Sun, J., Liu, C.-Z., Tappe, S., Kostrovitsky, S.I., Fu-Yuan, Wu., Yakovlev, D., Yue-Heng, Yang, Jin-Hui, Yang, 2014. Repeated kimberlite magmatism beneath Yakutia and its relationship to Siberian flood volcanism: insights from in situ U-Pb and Sr-Nd perovskite isotope analysis. Earth Planet. Sci. Lett. 404, 283–295.
Sun, J., Tappe, S., Kostrovitsky, S.I., Liu, C.-Z., Skuzovatov, S.Yu., Wu, F.-Y., 2018. Mantle sources of kimberlites through time: A U-Pb and Lu-Hf isotope study of zircon megacrysts from the Siberian diamond fields. Chem. Geol. 479, 228–240. https://doi.org/10.1016/j.chemgeo.2018.01.013.
Tappe, S., Steenfelt, A., Nielsen, T.F.N., 2012. Asthenospheric source of Neoproterozoic and Mesozoic kimberlites from the North Atlantic craton, West Greenland: New high-precision U-Pb and Sr–Nd isotope data on perovskite. Chem. Geol. 320–321, 113–127.
Tappe, S., Pearson, D.G., Prelevic, D., 2013. Kimberlite, carbonatite, and potassic magmatism as part of the geochemical cycle. Chem. Geol. 353, 1–3.
Tappe, S., Katie, A., Smart, K.A., Bogaard, P.V., 2015. 40Ar/39Ar Geochronology and Sr-Nd-Hf-Pb Isotope Systematics of Primitive Alkaline Basalts and Lamprophyres from the SW Baltic Shield. Geochim. Cosmochim. Acta. https://doi.org/10.1016/j.gca.2015.10.006.
Tappe, S., Brand, B.N., Stracke, A., Acken, D., Chuan-Zhou, Liu, Strauss, H.m., Wu, F.-Y., Luguet, A., Mitchell, R.H., 2016. Plates or plumes in the origin of kimberlites: U/Pb perovskite and Sr-Nd-Hf-Os-C-O isotope constraints from Superior craton. Chem. Geol. https://doi.org/10.1016/j.chemgeo.2016.08.19.
Yudin, D.C., Tomilenko, A.A., Travin, A.E., Agashev, A.E., Pokhilenko, N.P., Orihashy, Yu., 2014. The age of intrusion of kimberlite pipe Udachnaya-eastern: U-Pb and 40Ar/39Ar data. Dokladi of Russian Acad. Sci. 455 (1), 91–93 (in Russian).
Ukhanov, A.V., Ryabchikov, I.D., Kharkiv, A.D., 1988. Lithospheric mantle of the Yakutian kimberlite province. Moscow: Science 286 (in Russian).
Van Straaten, B.I., Kopylova, M.G., Russell, J.K., Webb, K.J., Scott Smith, B.H., 2008. Discrimination of diamond resource and non-resource domains in the Victor North pyroclastic Kimberlite, Canada. J Volcanol Geoth Res. 17, 128–138.
Wilson, L., Head III, J.W., 2007. An integrated model of kimberlite ascent and eruption. Nature 447, 53–57.
Woodhead, J., Hergt, J., Phillips, D., Paton, C., 2009. African kimberlites revisited: in situ Sr-isotope analysis of groundmass perovskite. Lithos 112, 311–317.
Wyatt, B.A., Baumgartner, M., Anckar, E., Grutter, H., 2004. Compositional classification of kimberlitic and non-kimberlitic ilmenite. Lithos 77, 819–840.
Hong-Fu, Zhang, Menzies, M.A., Mattey, D.P., Hinton, R.W., Gurney, J.J., 2001. Petrology, mineralogy and geochemistry of oxide minerals in polymict xenoliths from the Bultfontein kimberlites, South Africa: implication for low bulk-rock oxygen isotopic ratios. Contrib. Mineral. Petrol. 141, 367–379.